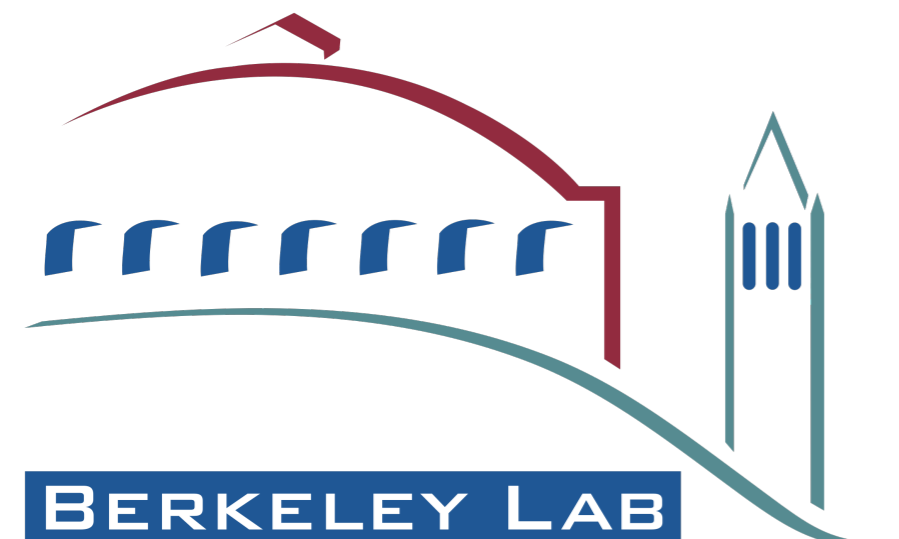


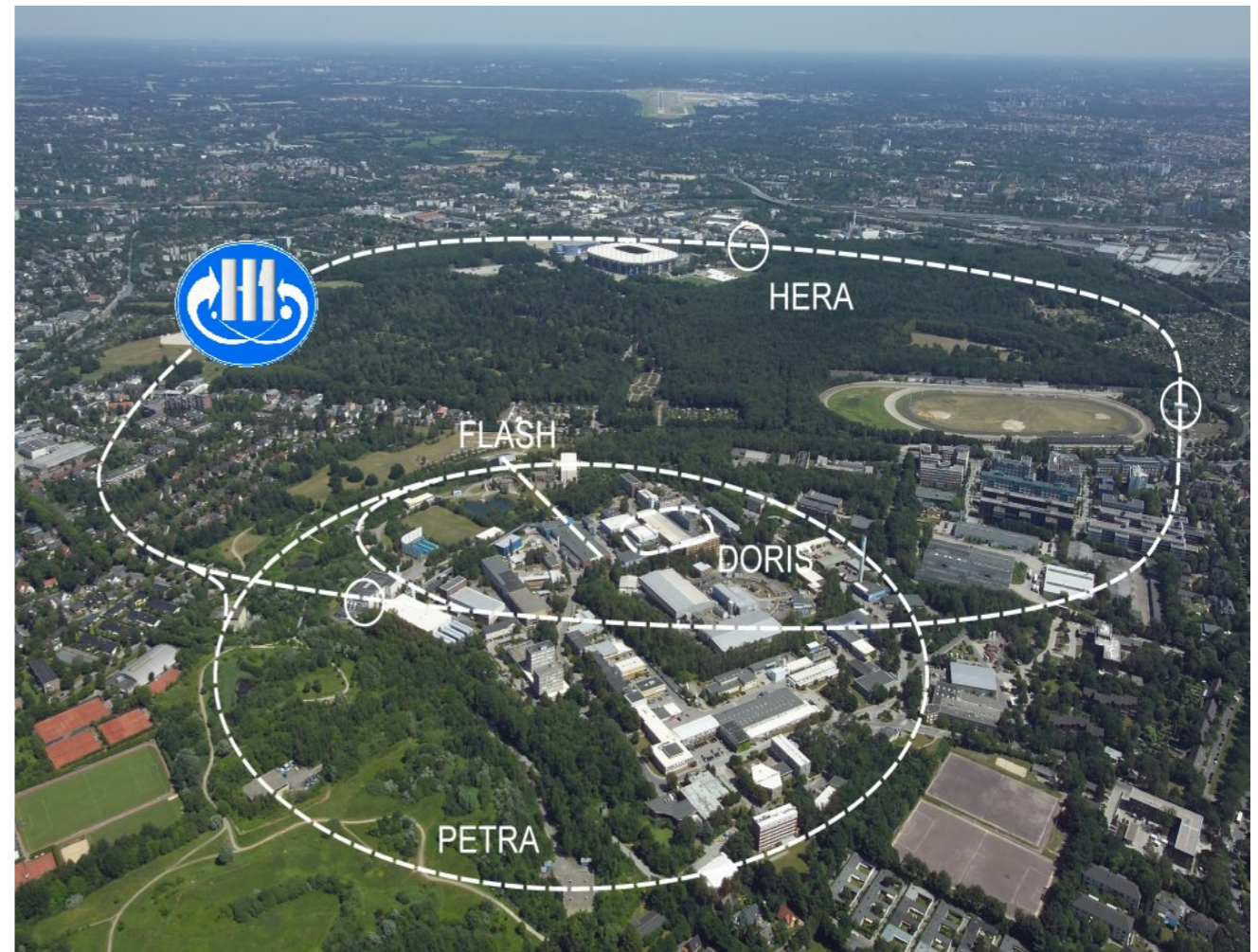
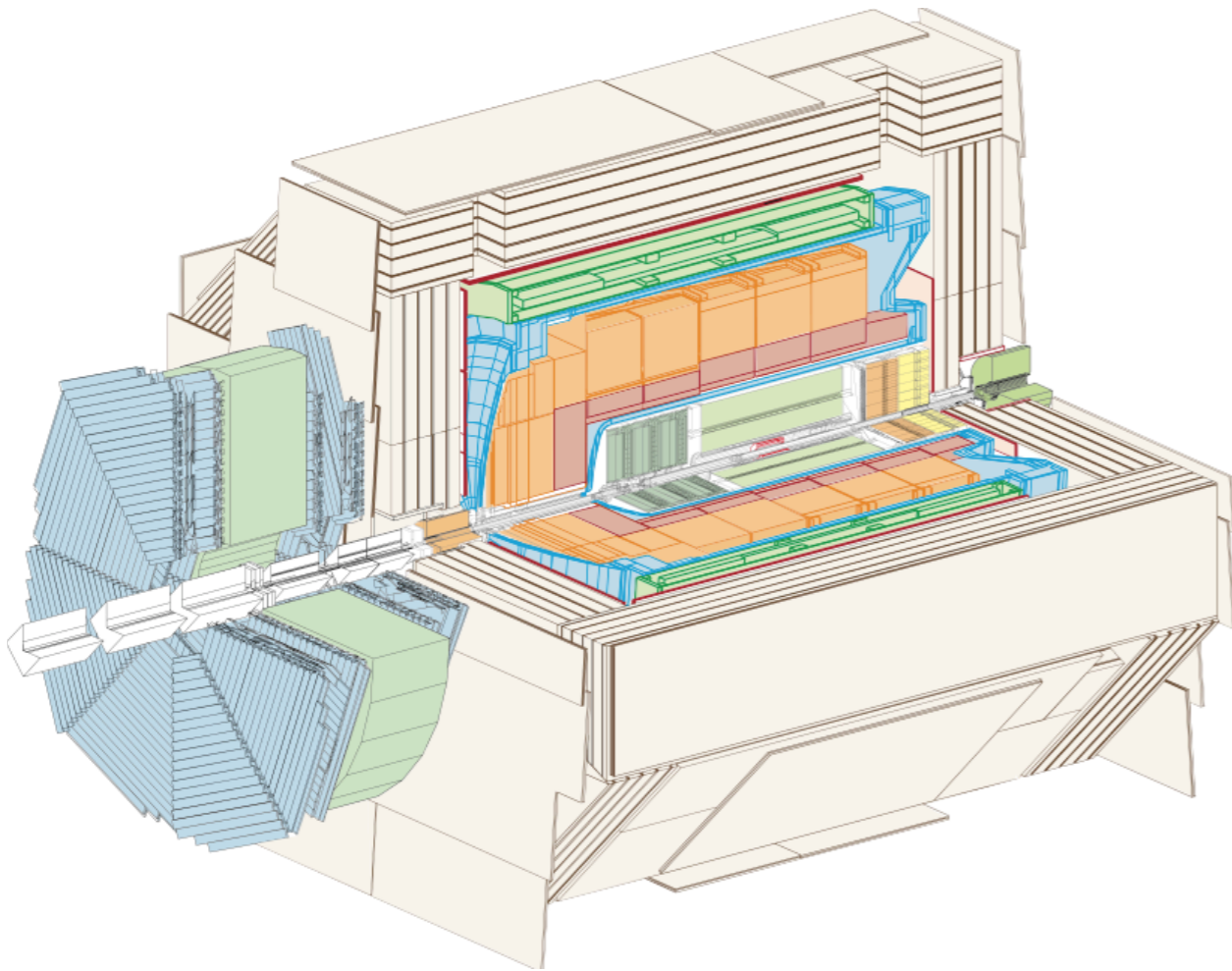
Lepton-Jet Azimuthal Asymmetry in H1 using MultiFold

Fernando Torales Acosta
Benjamin Nachman

on behalf of the H1 Collaboration



H1 at HERA



- **H1 Detector at the positron-proton collider, HERA. Hosted in Hamburg Germany**
- **Major goal was to study internal structure of the proton through deep inelastic scattering**

$$e(k) + q(p_1) \rightarrow e'(k_\ell) + jet(k_J) + X$$

Lepton Jet Asymmetry

Key Ingredients:

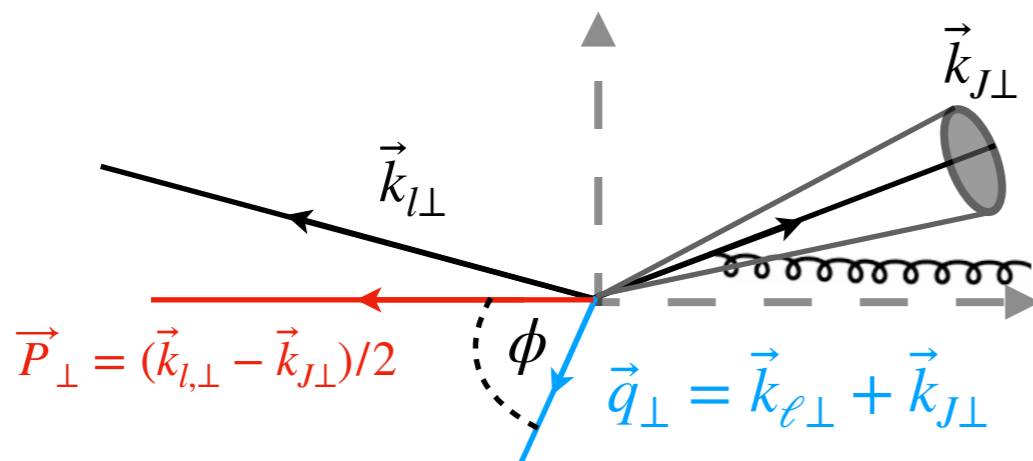
- $q_{\perp} = \text{Total}$ transverse momentum
- $P_{\perp} =$ Transverse momentum **difference**
- $\phi =$ Angle between q_{\perp} and P_{\perp}

$$\vec{q}_{\perp} = \vec{k}_{\ell\perp} + \vec{k}_{J\perp}$$

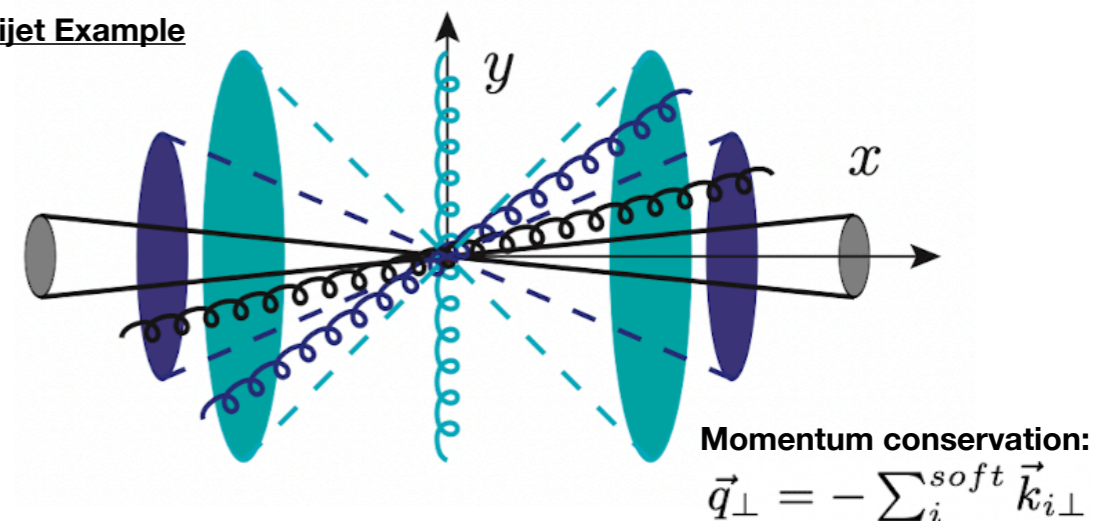
$$\vec{P}_{\perp} = (\vec{k}_{\ell\perp} - \vec{k}_{J\perp}) / 2$$

$$\phi = \text{acos}[(\vec{q}_{\perp} \cdot \vec{P}_{\perp}) / q_{\perp} P_{\perp}]$$

$$\cos(\phi) = (\vec{q}_{\perp} \cdot \vec{P}_{\perp}) / q_{\perp} P_{\perp}$$



Dijet Example

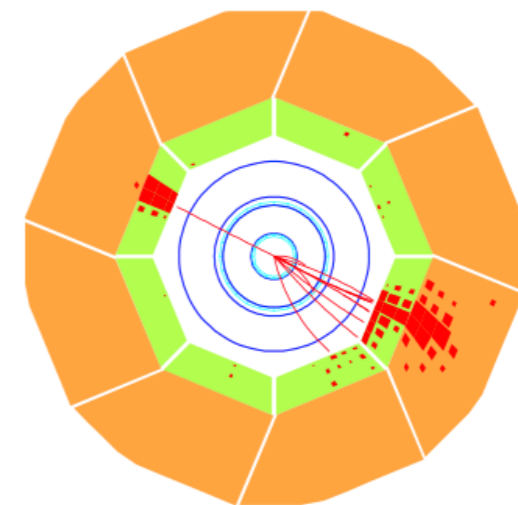
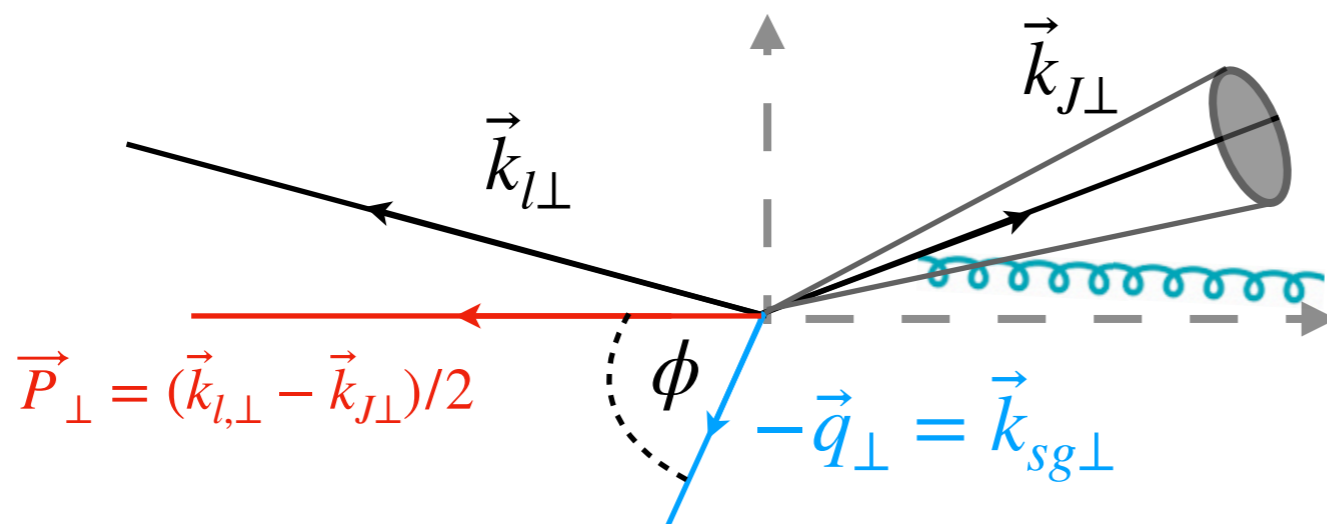


k_i , and therefore q_{\perp} will tend to point in the direction of the jet
Darker colors indicate probability of gluon emission

Lepton Jet Measurement

- Total transverse momentum of the outgoing system $\vec{q}_\perp = \vec{k}_{\ell\perp} + \vec{k}_{J\perp}$, is typically *small but nonzero*
 - Significant interest in studying transverse momentum dependent (TMD) parton distributions
- Imbalance can come from soft gluon radiation
 - soft gluon with momentum $k_{\perp g}$
 - unrelated to TMDs or intrinsic transverse momentum of target gluons
- Depending on kinematics, soft gluon radiation can dominate
 - Radiative corrections enhanced approximately as $(\alpha_s \ln^2 P_\perp^2 / q_\perp^2)^n$

$$P_\perp \gg q_\perp$$



$$e(k) + q(p_1) \rightarrow e'(k_\ell) + jet(k_J) + X$$

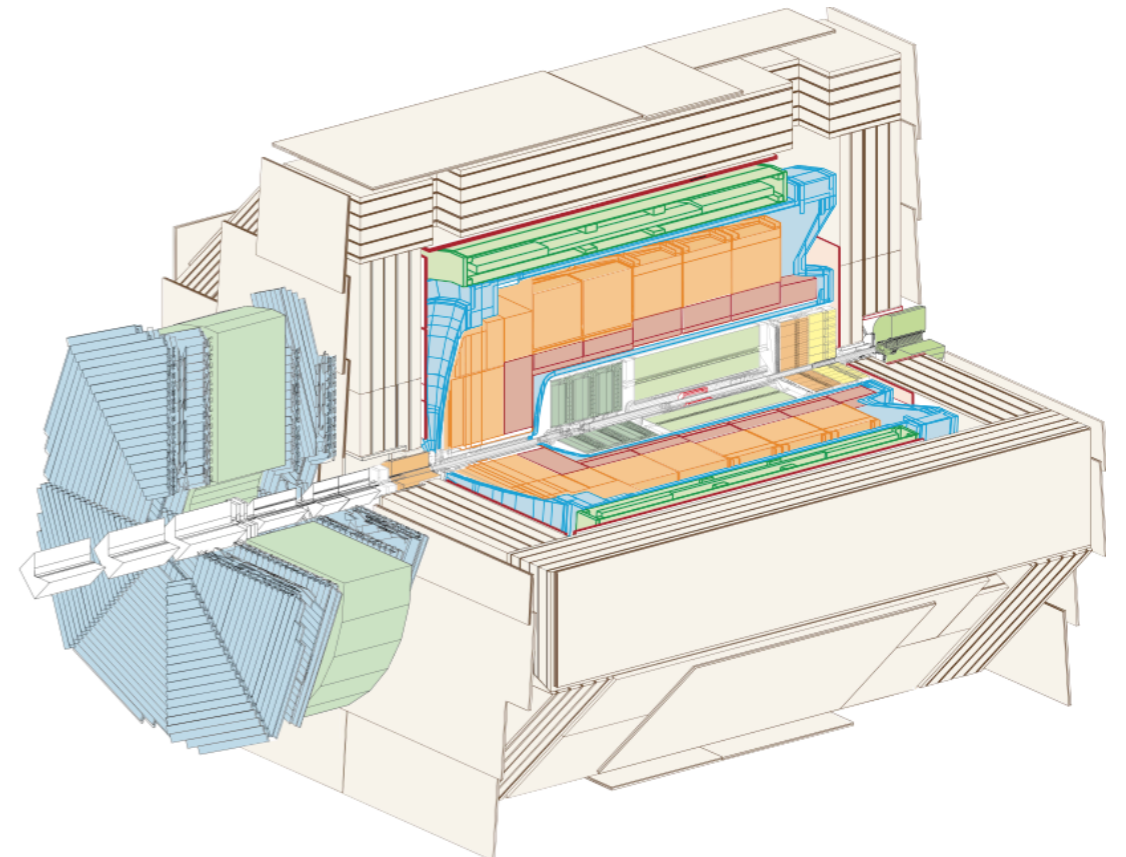
H1 Data

- Same data / selection / *unfolding* as [arXiv:2108.12376](https://arxiv.org/abs/2108.12376)
 - “Measurement of lepton-jet correlation in deep-inelastic scattering with the H1 detector using machine learning for unfolding”
- H1 Data from 2006 and 2007 periods at 130 pb^{-1}
 - Positron-proton collisions
- Fiducial Cuts:
 - $-1 < \eta_{\text{lab}} < 2.5$
 - $0.2 < y < 0.7$
 - $Q^2 > 150 \text{ GeV}^2$
 - $p_T^{\text{jet}} > 10 \text{ GeV}$
 - $k_T, R = 1.0$
 - $q_{\perp}/Q < 0.25$
 - $q_{\perp}/p_{T,\text{jet}} < 0.3$

Taking the *leading jet*

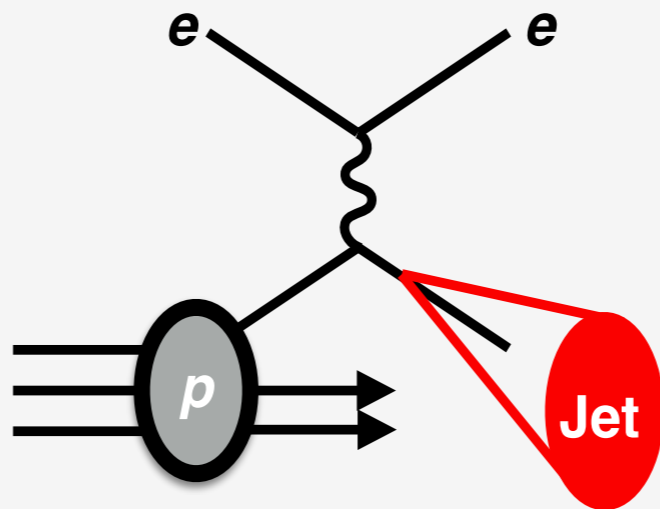
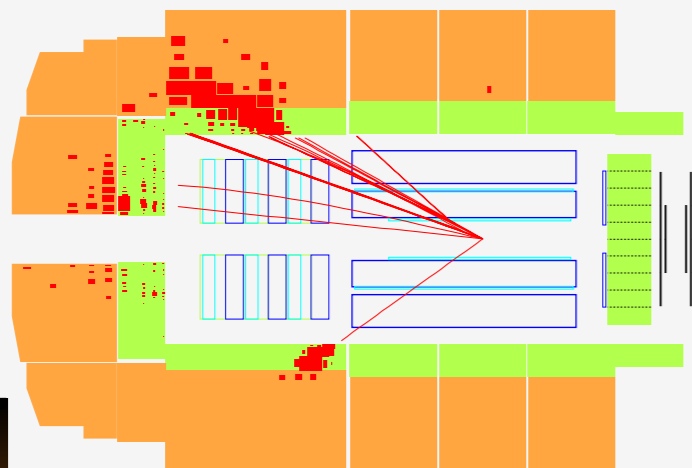
Cut on $q_{\perp}/p_{T,\text{jet}}$ to satisfy $P_{\perp} \gg q_{\perp}$:

$$p_{T,\text{jet}} \approx P_{\perp}/2$$



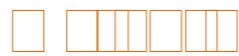
$$\sqrt{s} = 320 \text{ GeV}$$

MultiFold



2 step iterative approach

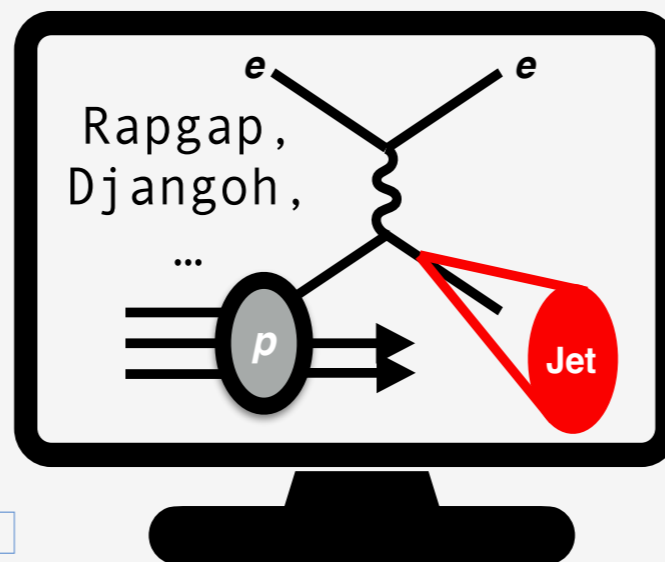
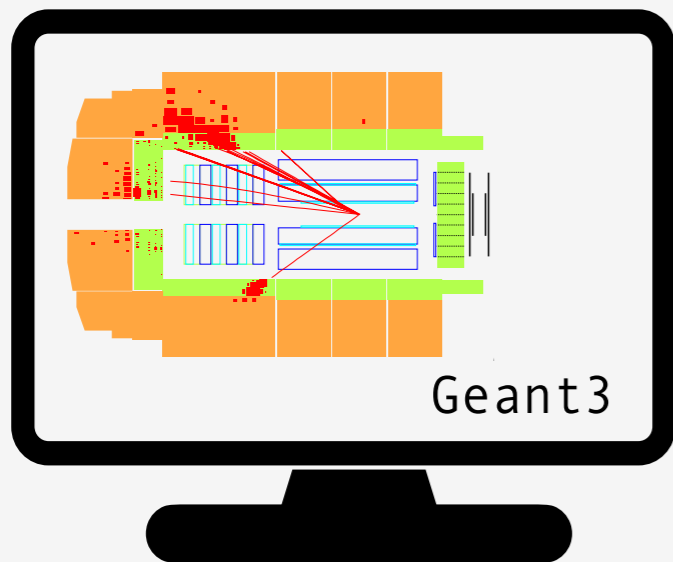
- Simulated events after detector interaction are re-weighted to match the data
- Create a “new simulation” by transforming weights to a proper function of the generated events






Machine learning is used to approximate 2 likelihood functions:

Reco MC to Data
reweighting

Previous and new Gen
reweighting

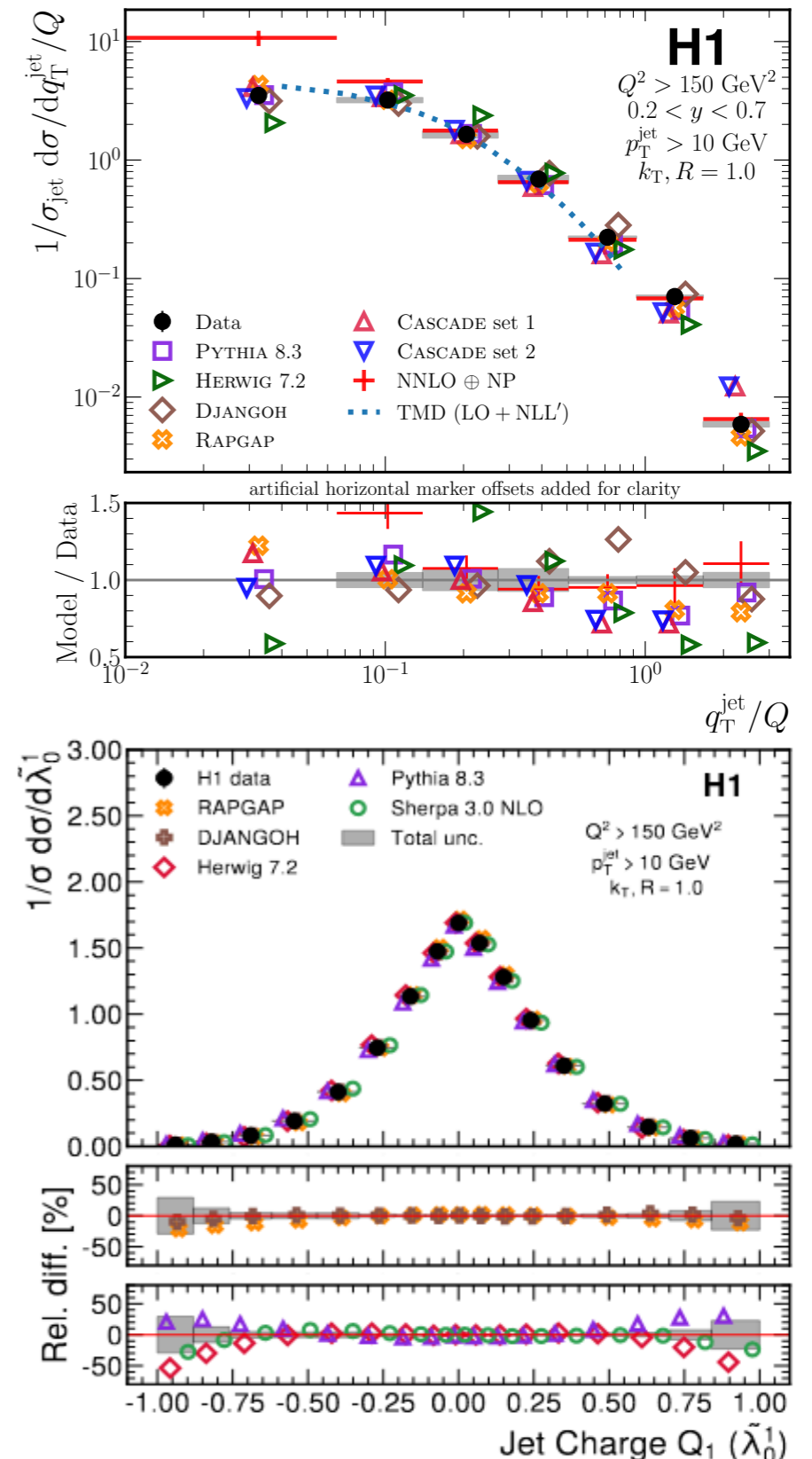


MultiFold Overview

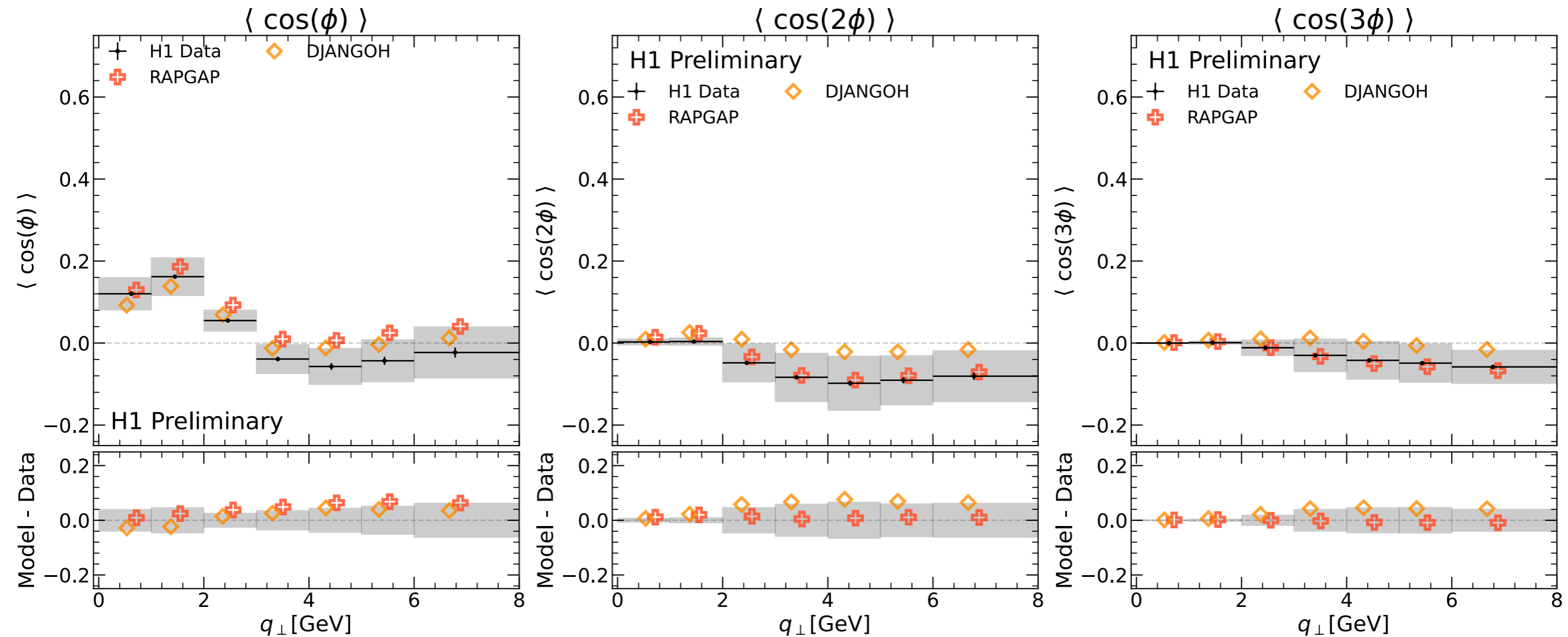
- Multi-dimensional, un-binned unfolding result
 - Lepton-Proton momentum imbalance
 - PhysRevLett.128.132002 
- Jet constituent-level unfolding
 - Un-binned Deep Learning unfolding of Jet Substructure
 - [arXiv 2303.13620](https://arxiv.org/abs/2303.13620) 
- Recycling of unfolded event weights
 - And measure *moments* 

Multifold previously used to unfold:

$$p_x^e, p_y^e, p_z^e, p_T^{\text{jet}}, \eta^{\text{jet}}, \phi^{\text{jet}}, \Delta\phi^{\text{jet}}, q_T^{\text{jet}}/Q$$

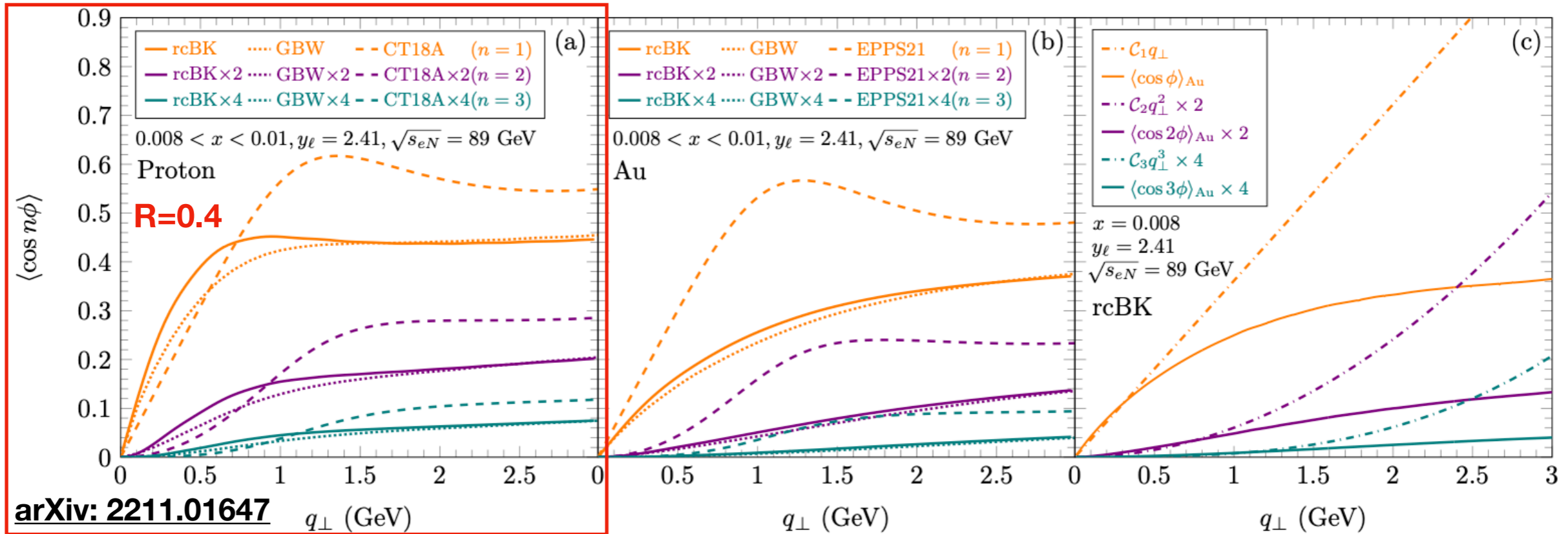


H1 Unfolded Data



- Leading moment is $\langle \cos(\phi) \rangle$, expected in lepton-jet events
- All harmonics approach 0.0 at higher q_{\perp} , may compromise $P_{\perp} \gg q_{\perp}$
- Rapgap and Django, tuned to HERA II data, exhibit good agreement
- Note *small absolute* value of central values

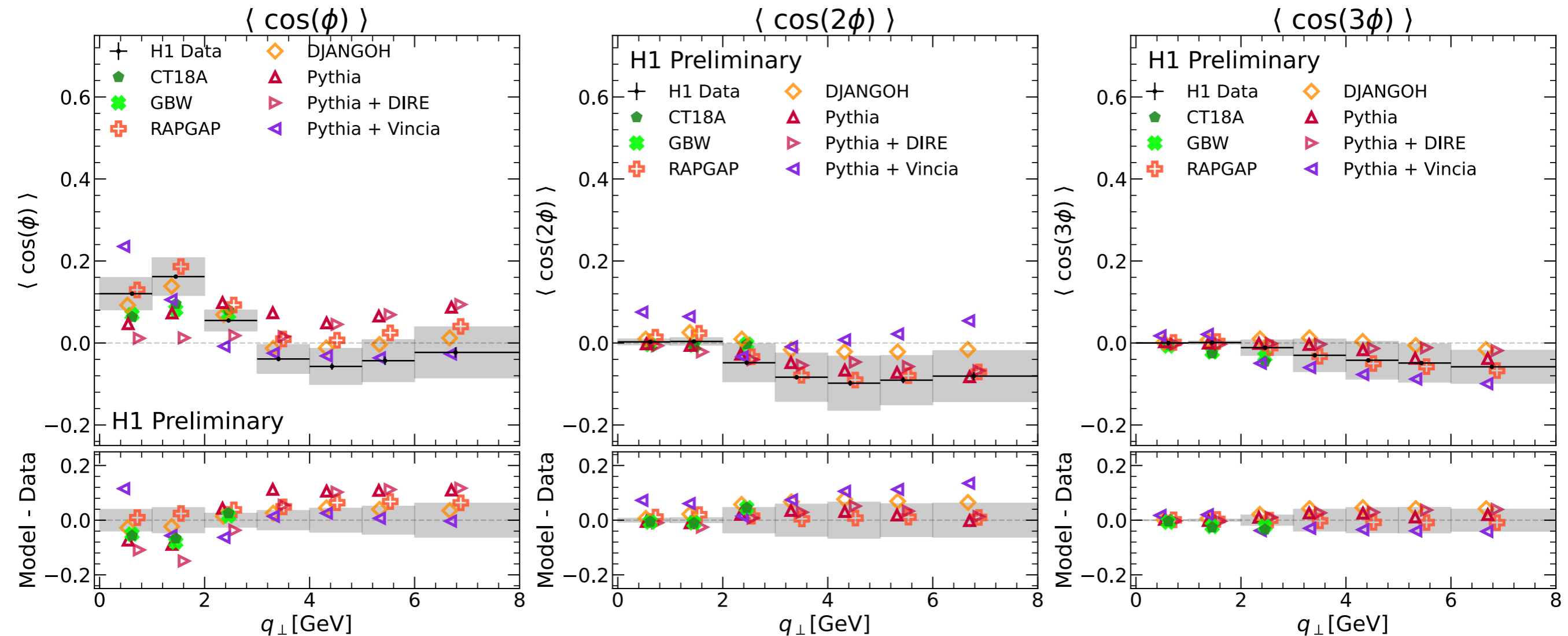
Even more interesting at EIC!



$$\vec{q}_{\perp} = \vec{k}_{\ell\perp} + \vec{k}_{J\perp} \quad \vec{P}_{\perp} = (\vec{k}_{\ell\perp} - \vec{k}_{J\perp}) / 2$$

- **Asymmetry may be sensitive to Parton saturation effects (EIC)**
- GBW — Three parameter model fit to HERA data, input to $f(b, x)$
- Calculation in TMD framework with CT18A PDF
- **Recalculated to match HERA kinematics, with jet $R=1.0$**

H1 Unfolded Data



- **Three harmonics of the azimuthal angular asymmetry between the lepton and leading jet as a function of q_{\perp} .**
- **Predictions from multiple simulations as well as a pQCD calculation are shown for comparison.**
- **PYTHIA, not tuned to HERA II, performs inconsistently**

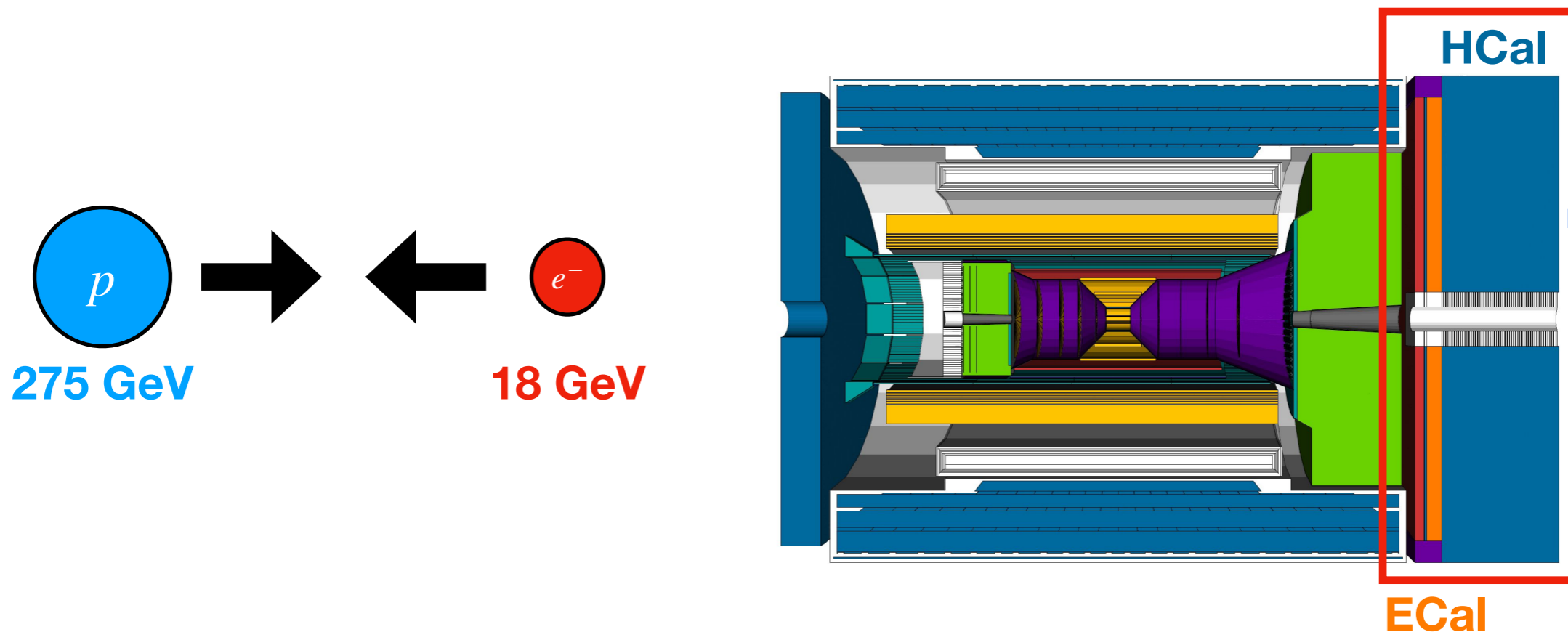
Conclusions

- Promising measurement probing soft gluon radiation
 - Test of pQCD calculations
 - Important reference for lepton-jet DIS measurements
 - Reasonable agreement with Rapgap + Djangoh
- MultiFold
 - First recycling of unfolded event weights! Reusability is key
 - measurement of *moments*, requiring the *unbinned unfolding!*
- Outlook:
 - Because of H1's data + simulation conservation, we can use recent insights and advances in methodology to analyze ~15 year old data
 - Important Implications for studies at EIC, both in observable and methods

ML-Assisted Detector Optimization

Goal:
**best experimental design suited for the
best detector reconstruction**

Forward Hadronic Calorimeter

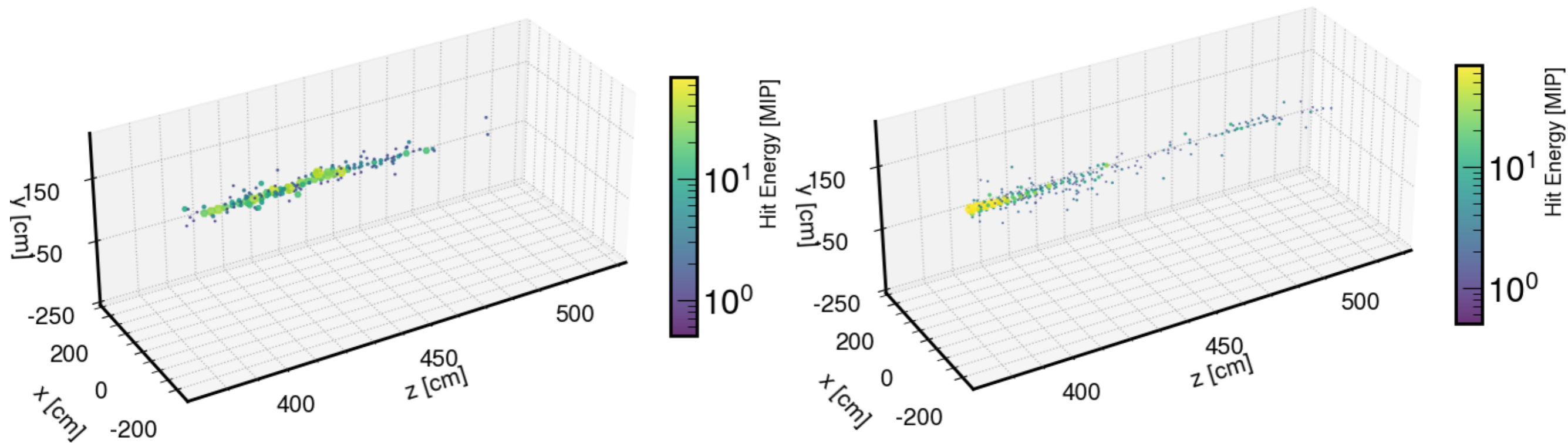


- The incoming proton/ion has a significantly larger kinetic energy than the incoming electron.
- If we want to measure *jets*, we need a granular, forward calorimeter
 - Forward region, $1.2 < \eta < 3.5$
- Deep Sets and GNNs for pion energy regression
- G4 approximation of *ePIC*

Figure Courtesy

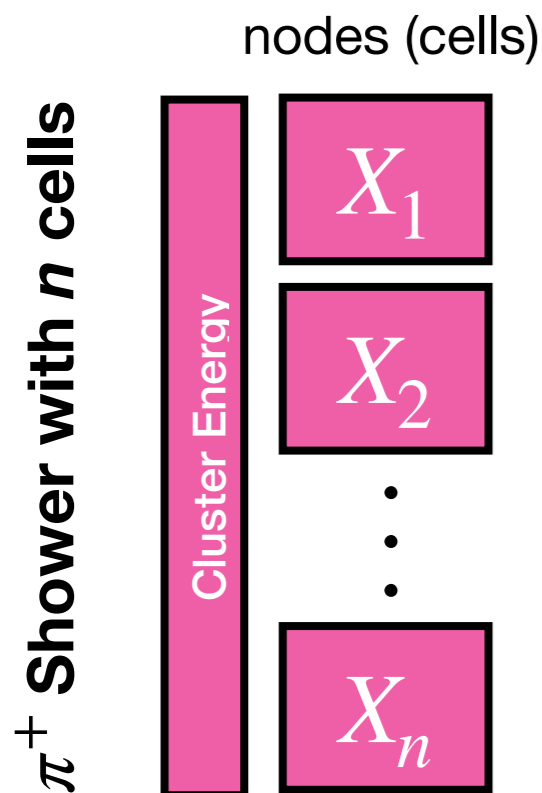
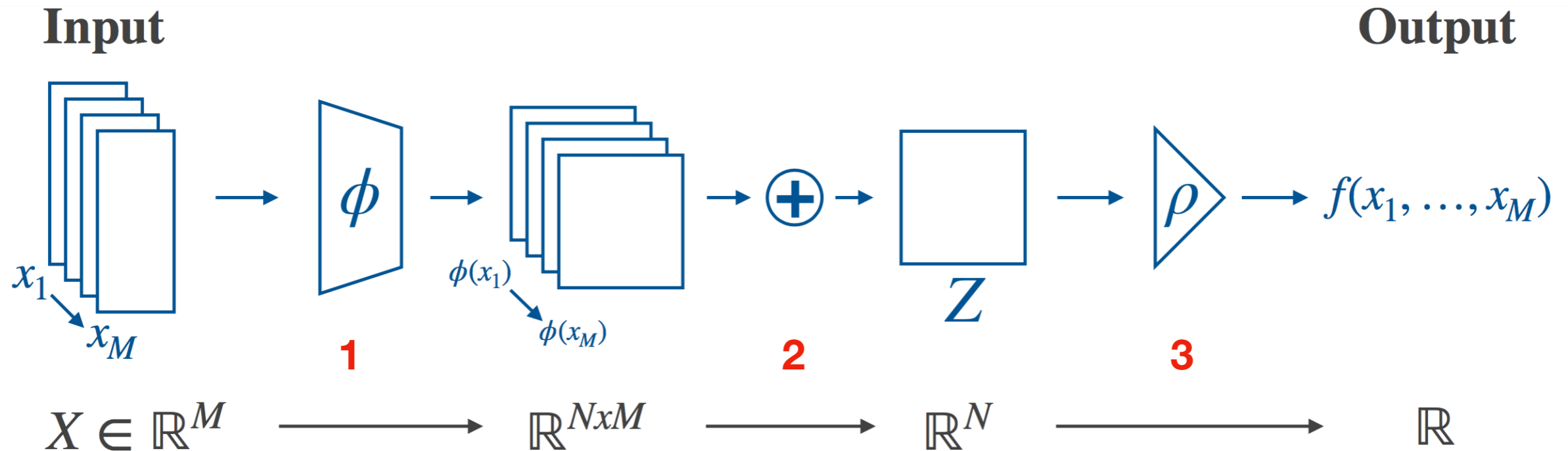


Detector Simulation and Reconstruction



- Geant4 Simulation of single π^+ showers
 $1 < P_{\text{Gen.}} < 125 \text{ GeV}/c$
- $\mathcal{O}100 - 1000$ Cell Hits per shower, **point clouds**
- Establish a model to predict $P_{\text{Gen.}}$ given cell information
- Condition model on position of longitudinal segmentation

Deep Sets



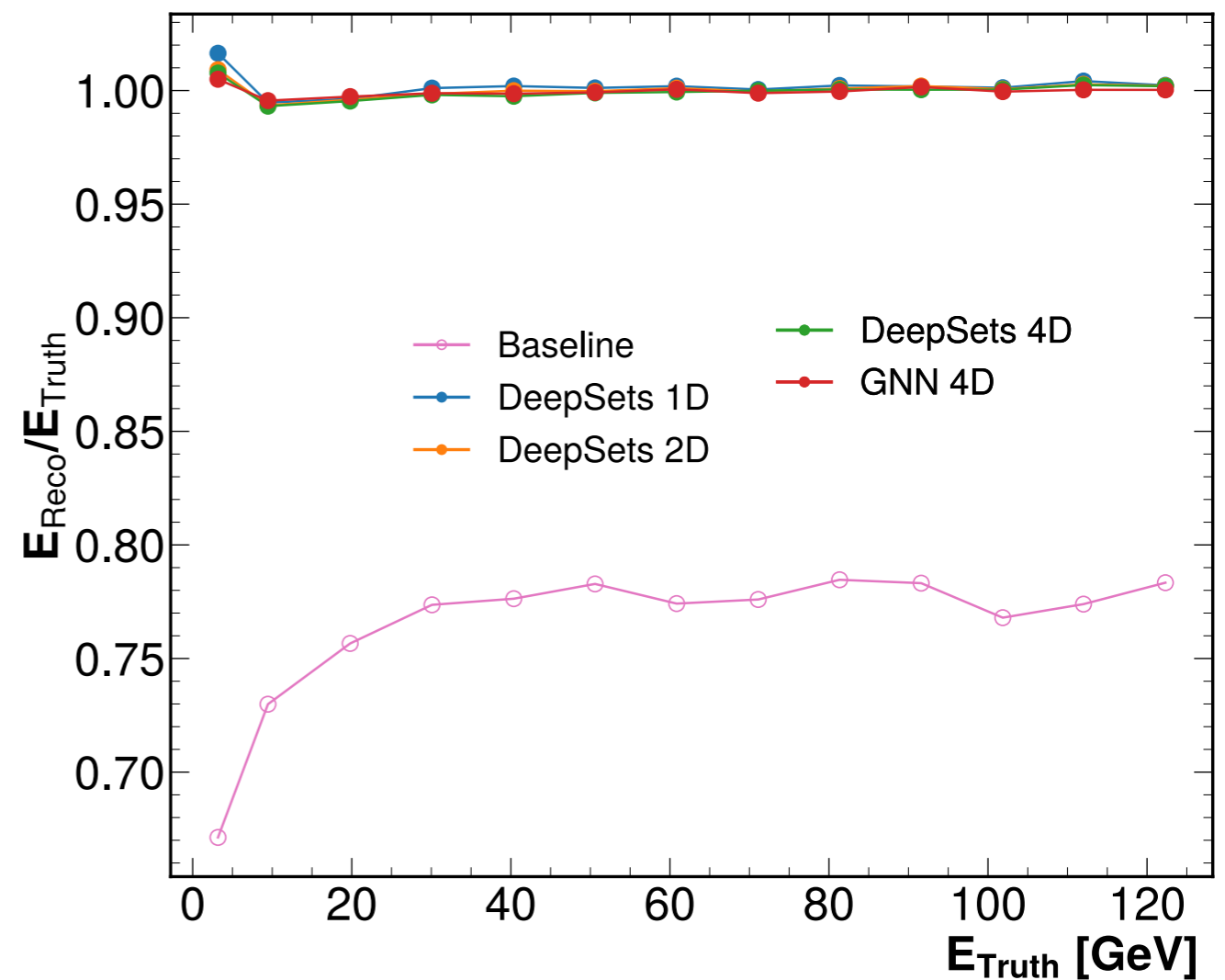
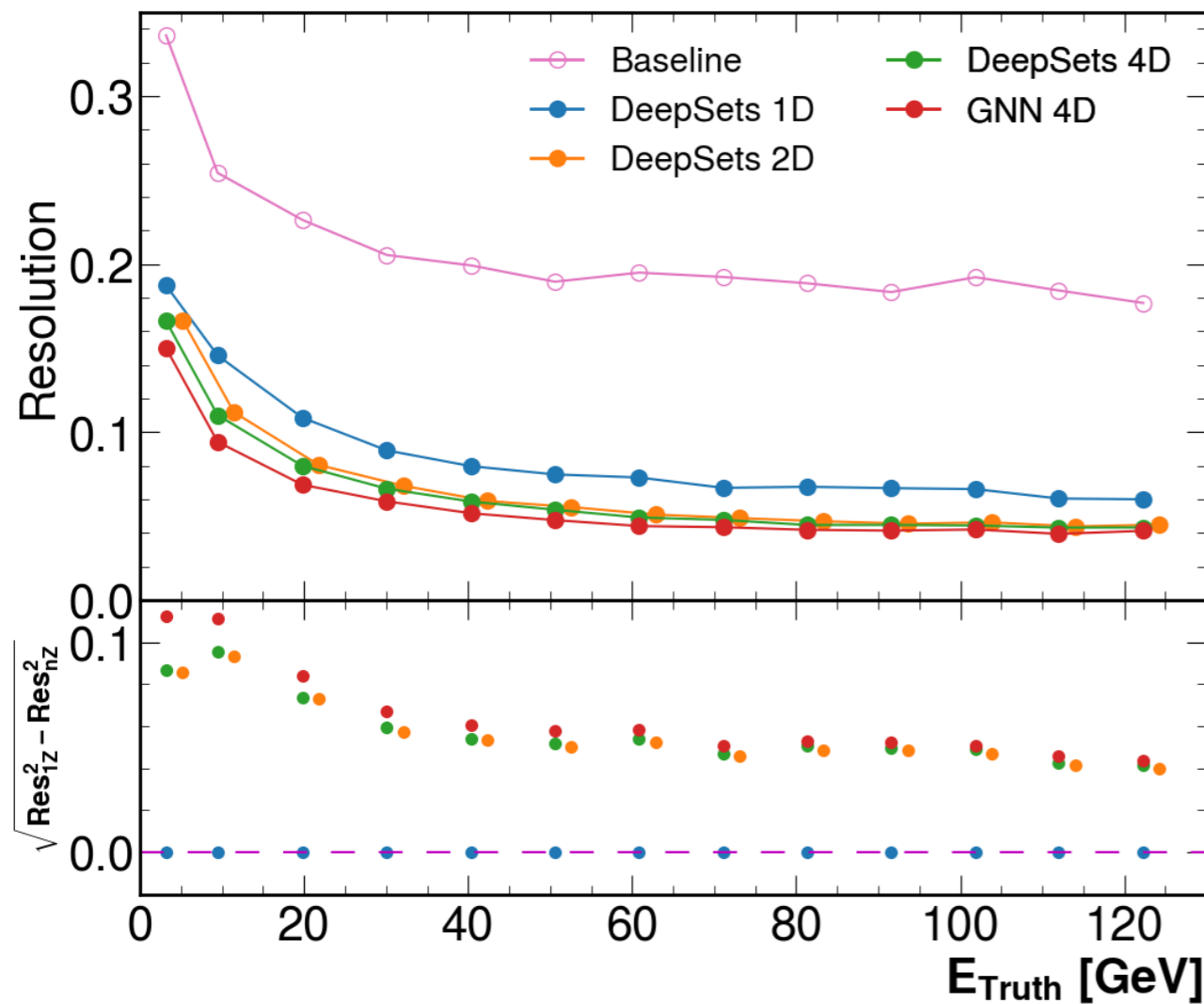
$$X_i = \left\{ \begin{array}{c} E \\ x \\ y \\ z \end{array} \right\} \in \mathbb{R}^4$$

1. Latent
2. Aggregation
3. Final Output

Goal:
 π^+ Energy
 Regression

Model uses energy and position information for energy regression

Energy Regression: Feature Dimension

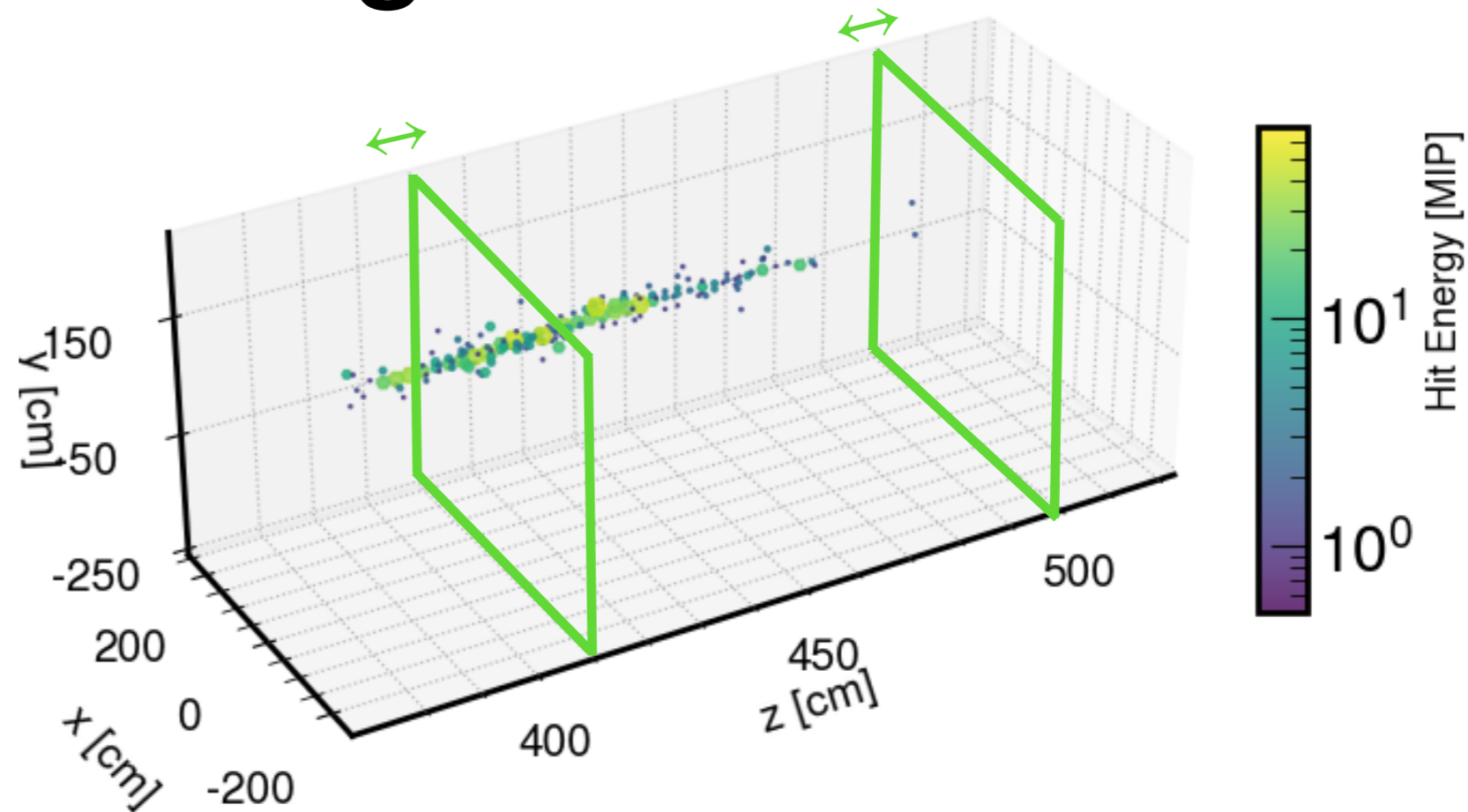


- Using DeepSets for regression, biggest improvement is the inclusion of cell-Z information
- Additional transverse information (2D \rightarrow 4D) less impactful
- Energy scale within %2 of truth

Data Processing for Models

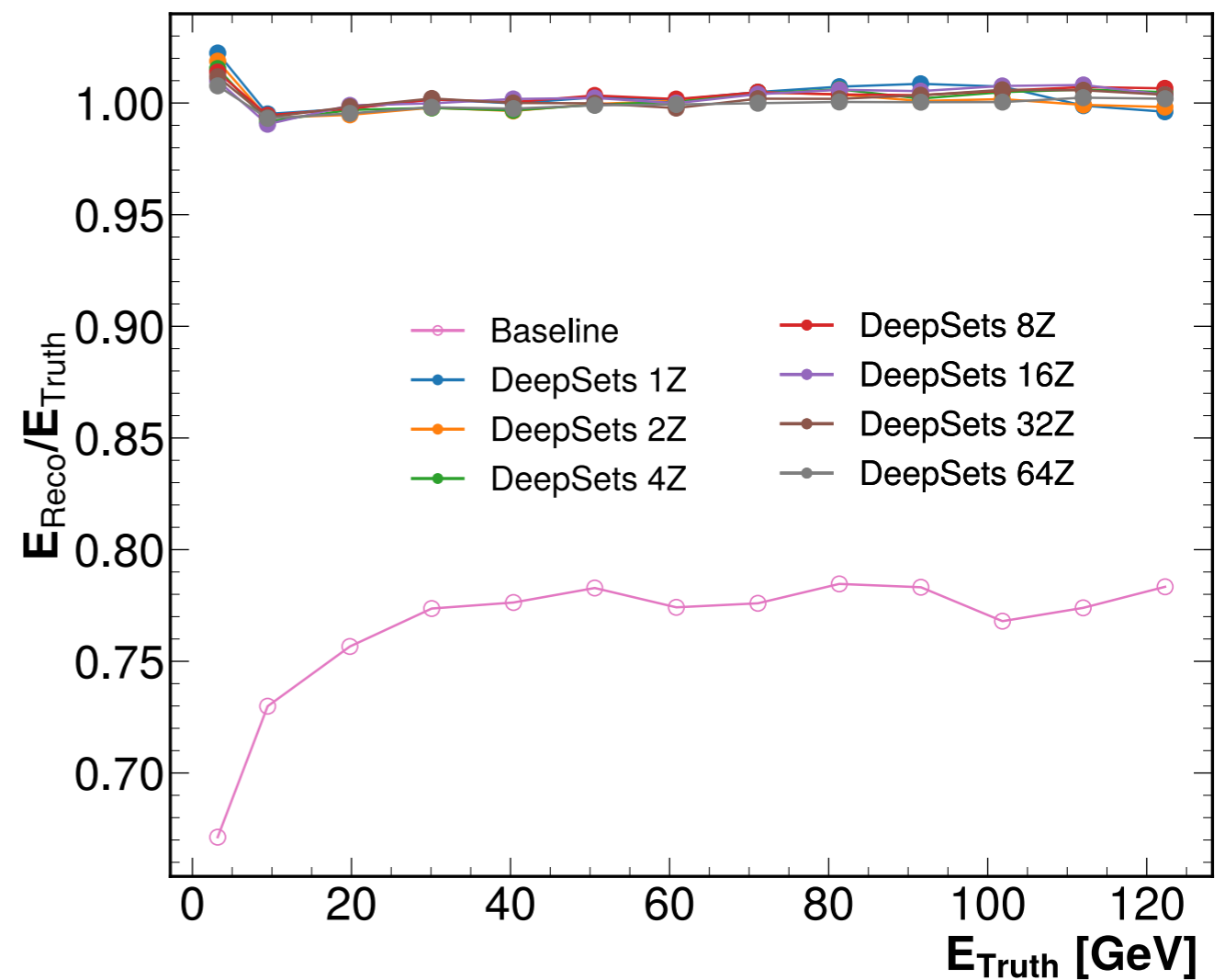
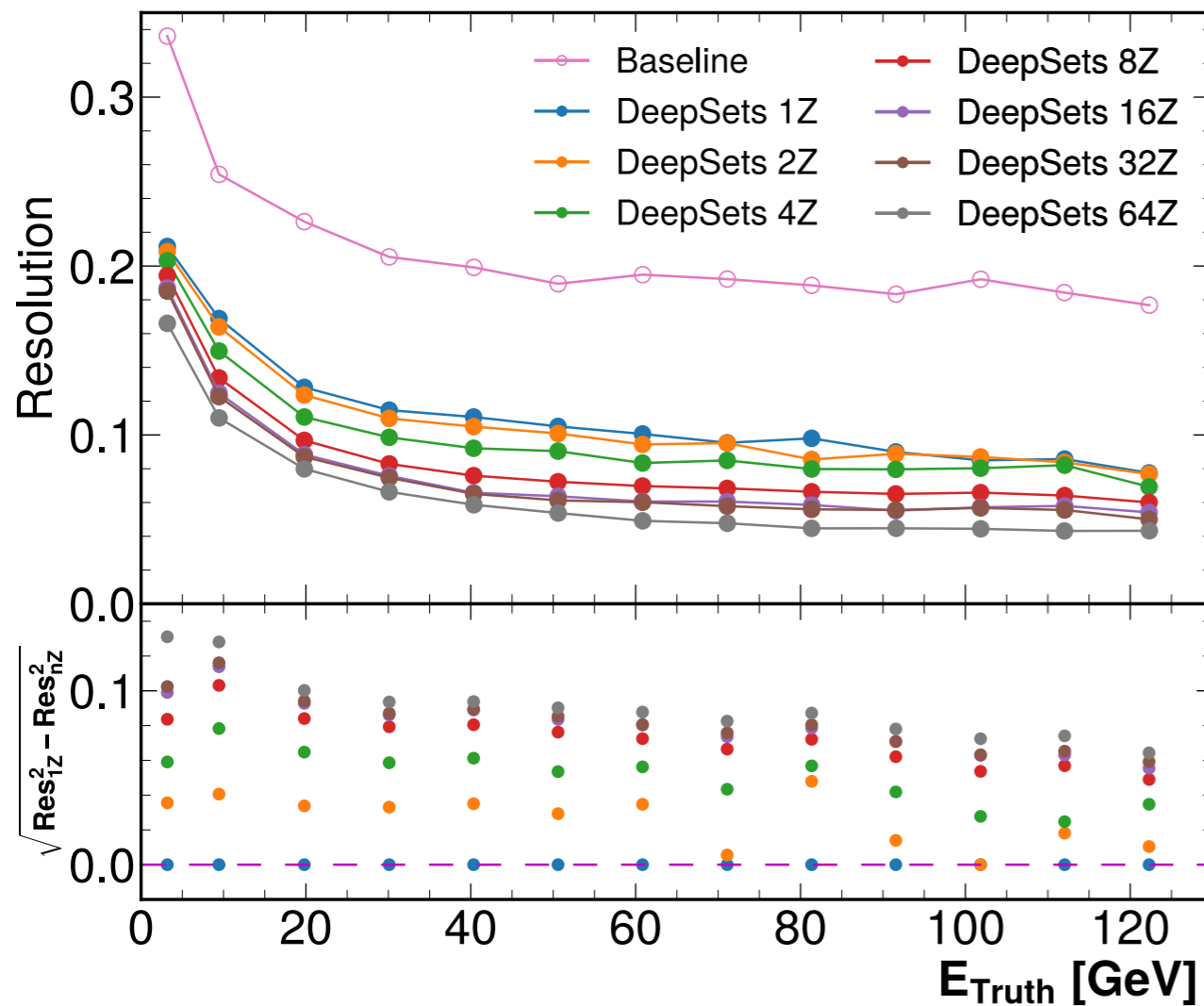


4-Layer Configuration



- Full point cloud readout is *unrealistic* for final detector
- Segment the calorimeter N=1-64 layers
- Run regression, identifying optimal longitudinal configuration

Energy Regression: Number of Layers



- 1-Layer configuration w/ Deepsets outperforms baseline
- Intuitive increase in performance as N_z increases
- Scale is insensitive N_z

Conclusions and Outlooks

- Longitudinal cell information yield greatest improvement. Resolution less sensitive to transverse segmentation
- Paper out this week!
 - *The Optimal use of Segmentation for Sampling Calorimeters*
- Next Step: Model conditioned directly on detector configuration

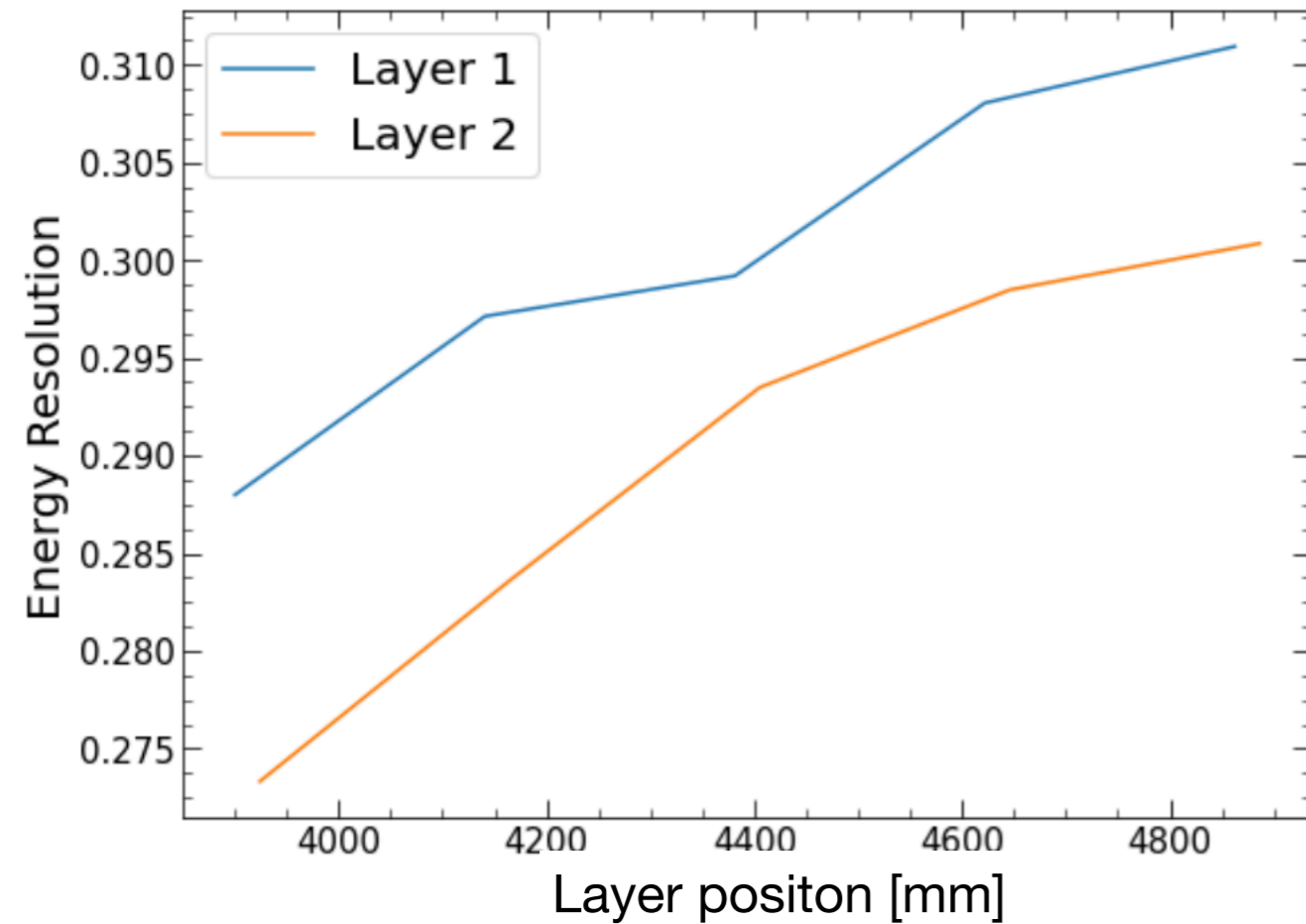
$$\sigma_E = f(z_1, z_2, \vec{x})$$

END... END

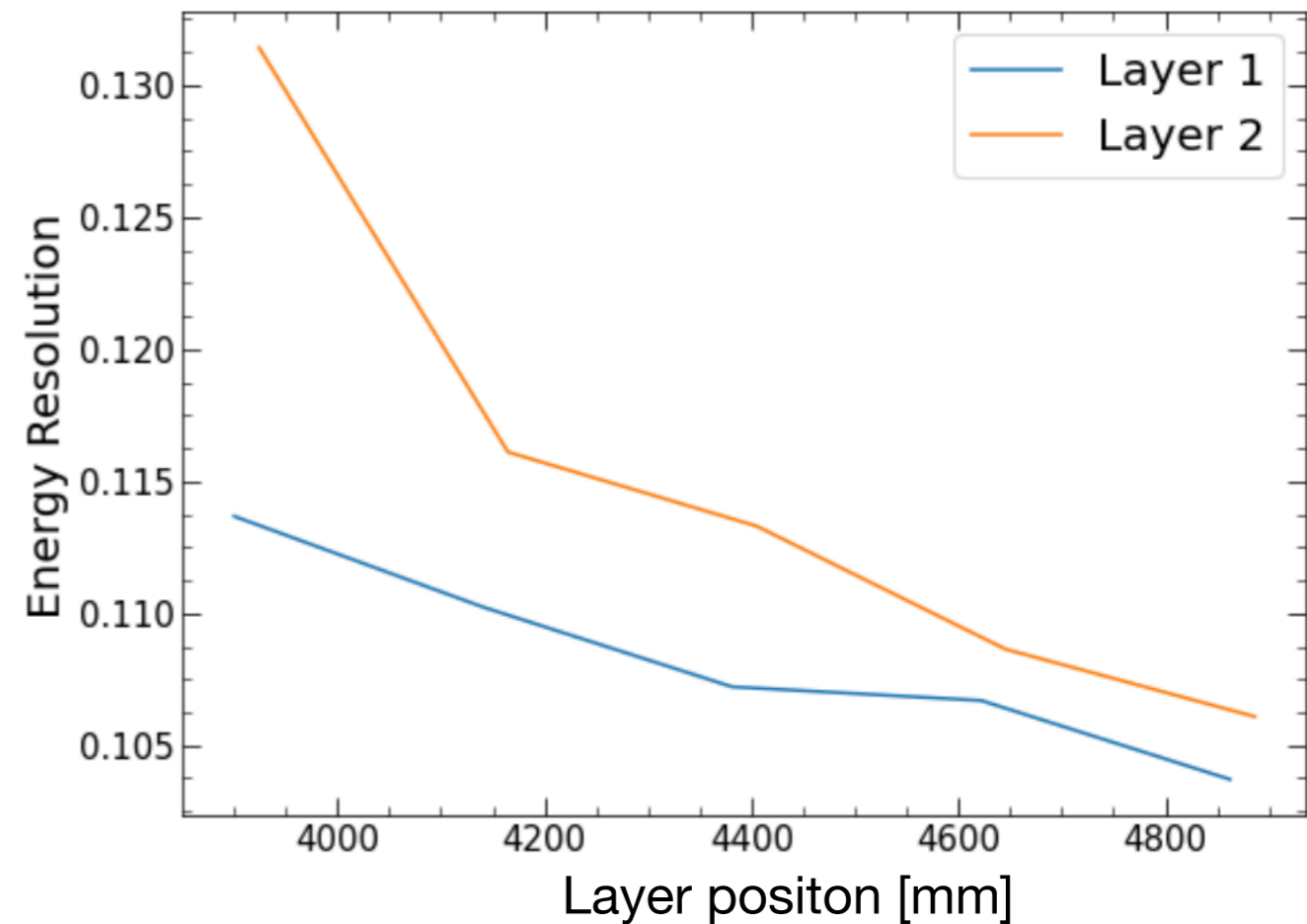
Backup

$$\sigma_E = f(z_1, z_2, \vec{x})$$

$P_{\text{Gen.}} < 10.0 \text{ GeV}/c$

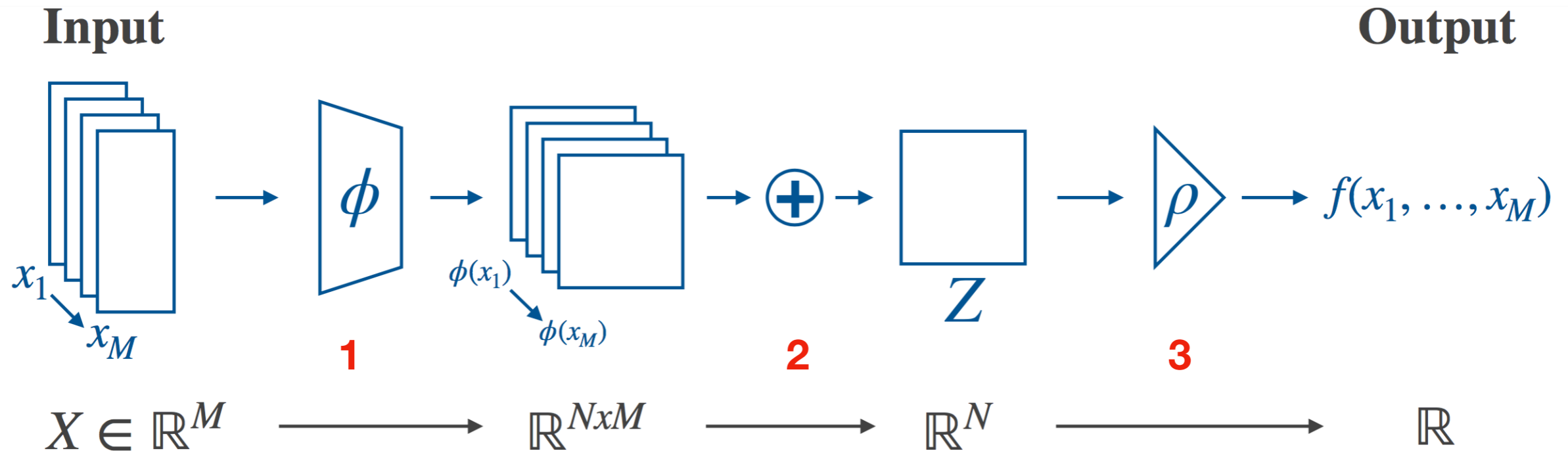


$P_{\text{Gen.}} > 50.0 \text{ GeV}/c$



We have a differentiable function for energy resolution

Deep Sets



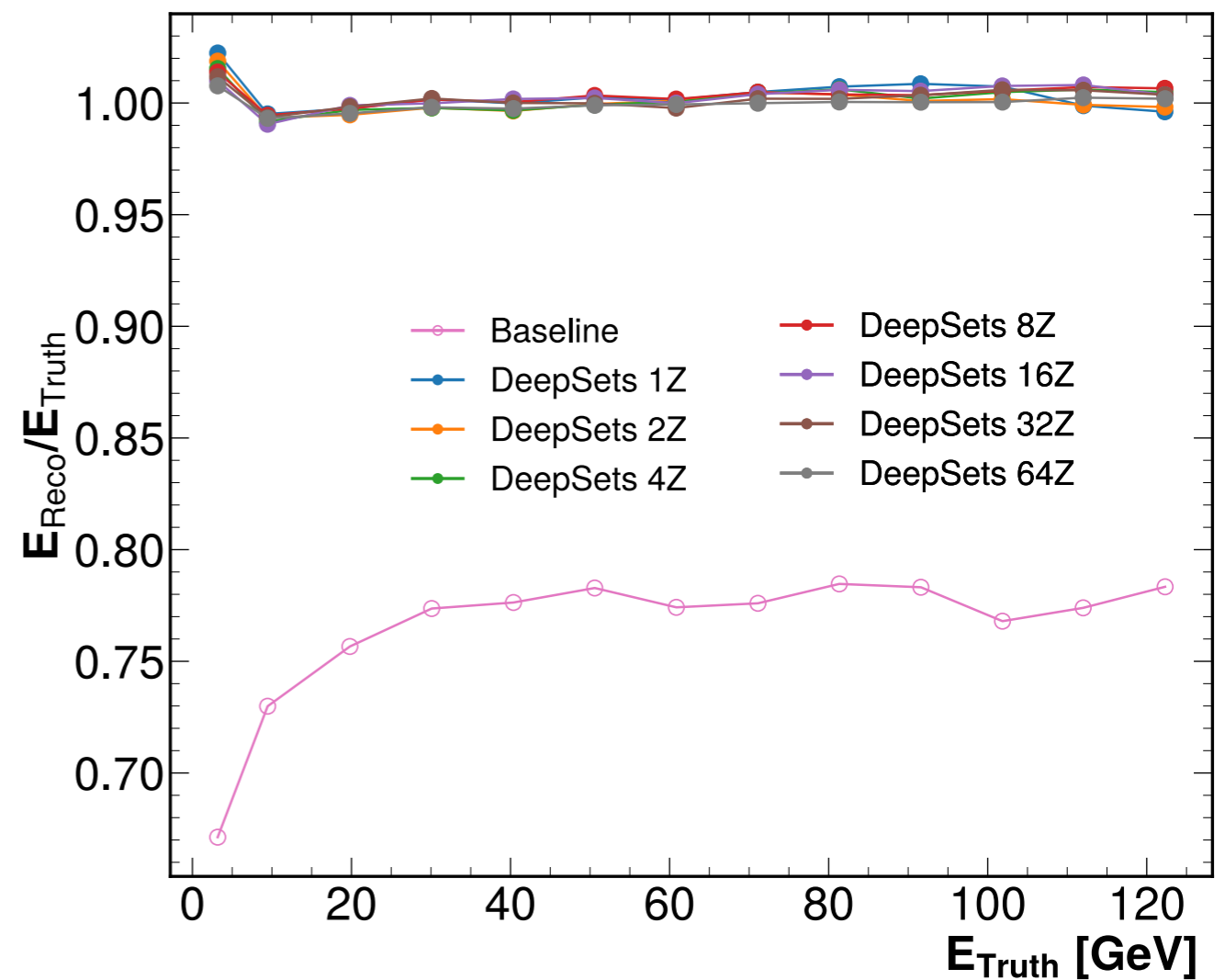
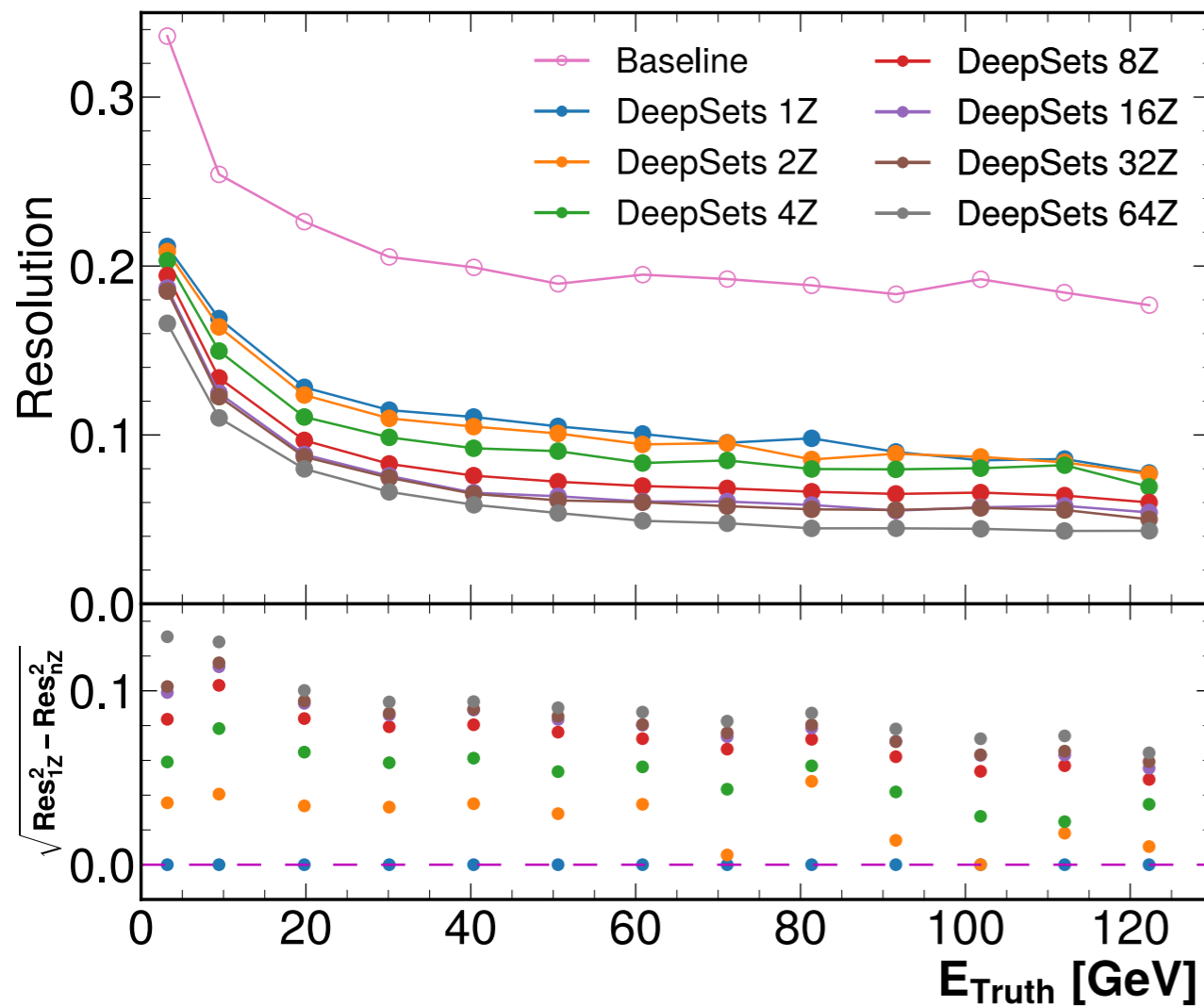
1. Transform inputs into some latent space
2. Destroy the ordering information in the latent space ($+$, μ)
3. Transform from the latent space to the final output

Permutation Invariant
Works well with point clouds
A GNN without edges

arXiv: 1703.06114

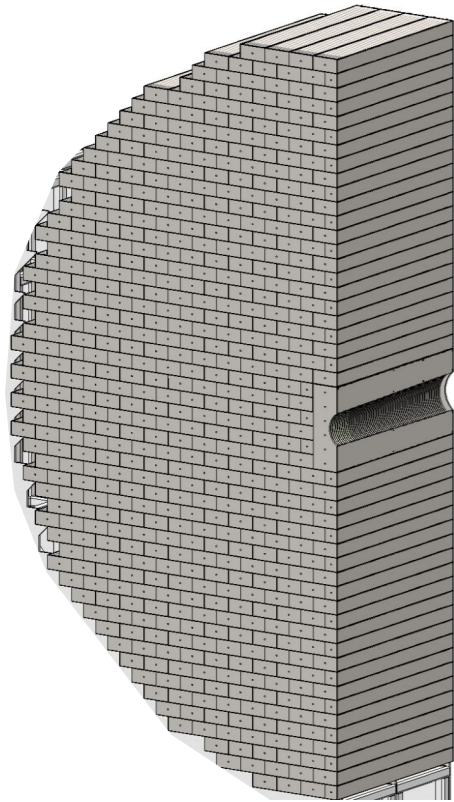
arXiv:1810.05165

Energy Regression Results



- Geant4 Simulation of single π^+ showers
- Condition model on position of longitudinal segmentation

Forward HCal



- High-granularity iron-scintillator calorimeter
- Forward region, $1.2 < \eta < 3.5$
- Sampling calorimeter comprised of 0.3 cm scintillator tiles sandwiched between 2.0 cm steel plates

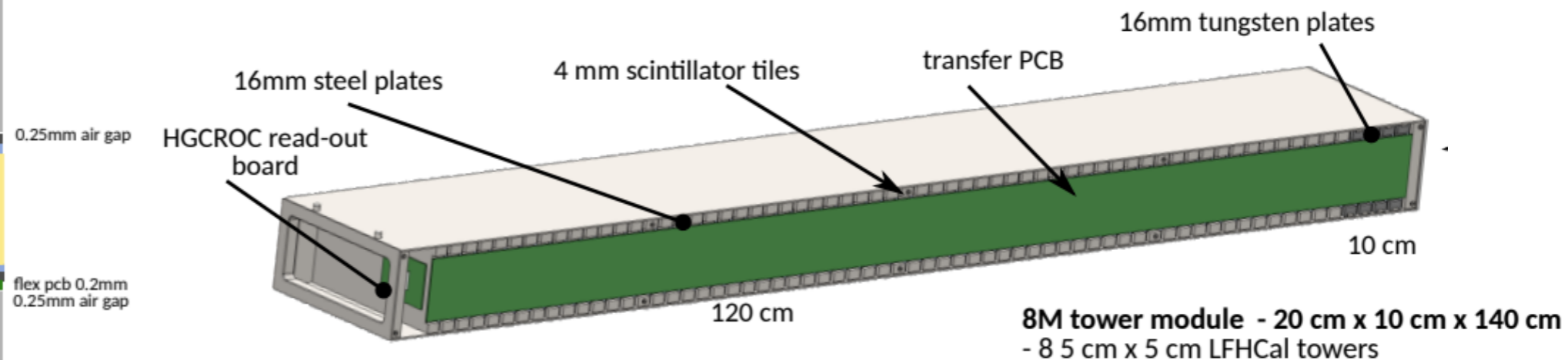
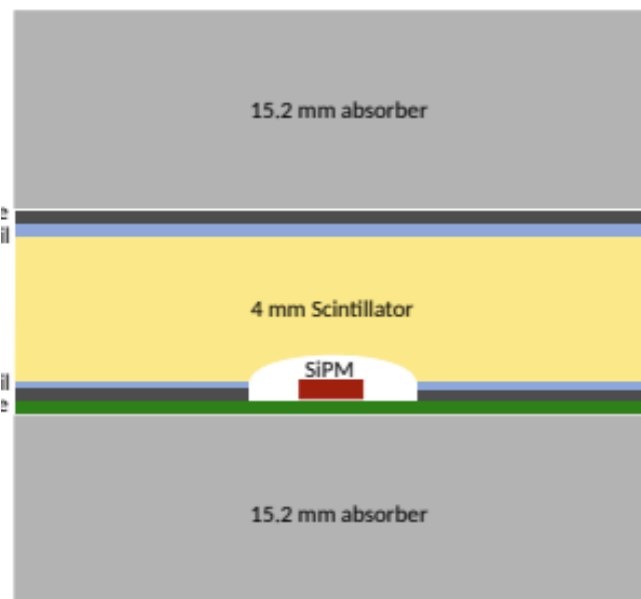


Figure Courtesy

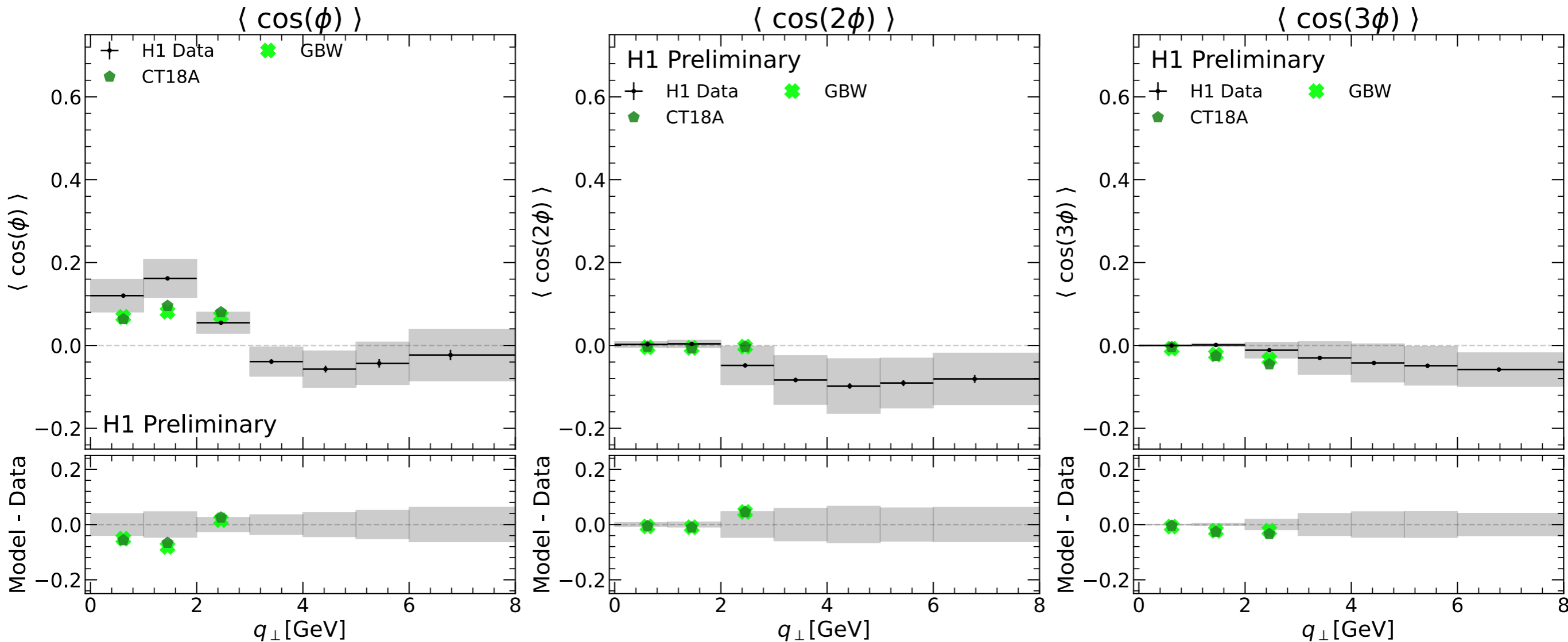


Observable Motivation

1. Probes soft gluon radiation $S(g)$
 - Soft gluon radiation can be the primary contribution to asymmetry for certain kinematics
 - Asymmetry is Perturbative, test pQCD calculations
2. May represent a vital reference for other signals, in particular TMD PDF measurements
 - Large interest in Lepton-Jet Correlations to probe TMDs
 - In TMD factorization framework, one can factorize contributions from transverse momentum dependent (TMD) PDFs and Soft gluon radiation
3. Observable is sensitive to gluon saturation phenomena, potentially measurable at the EIC

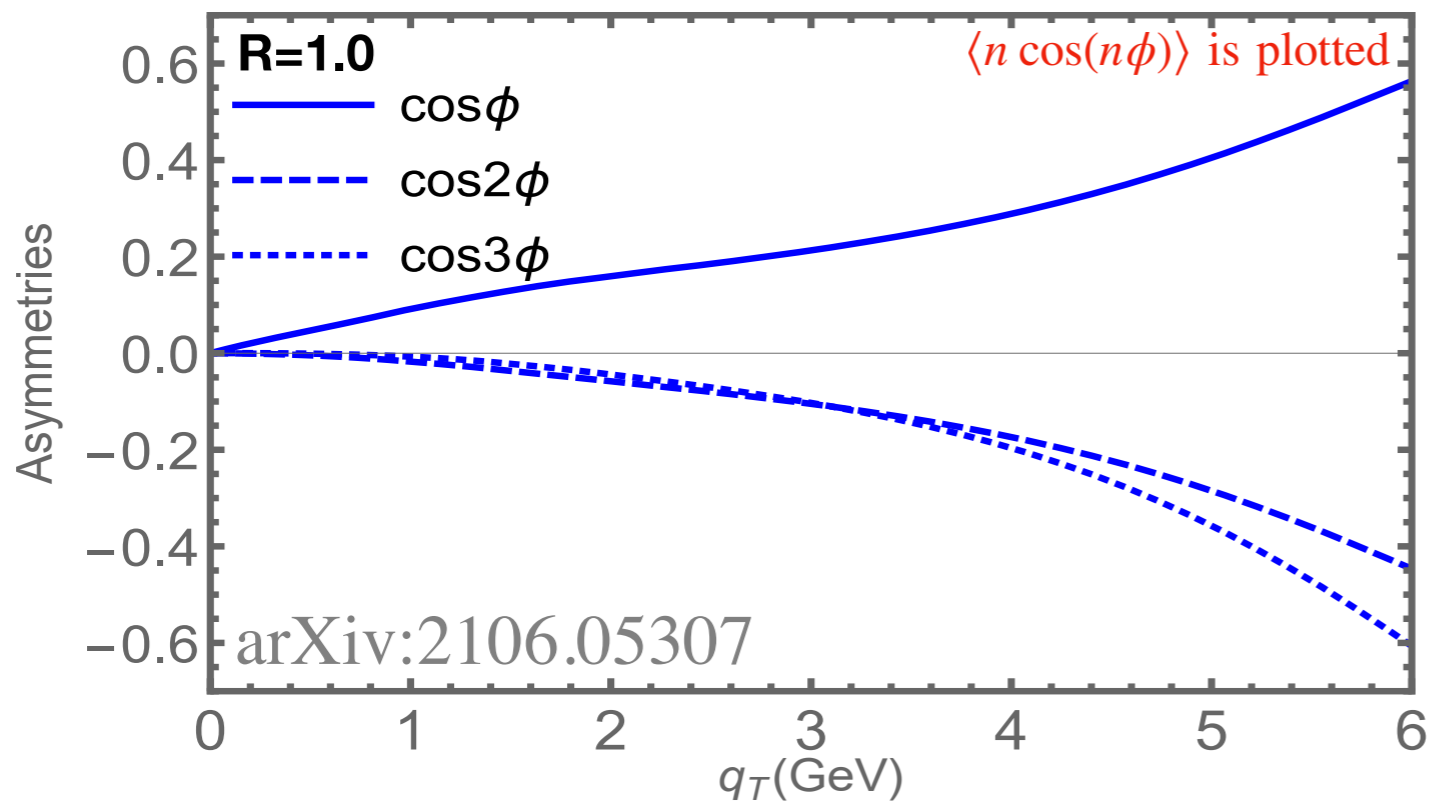
$$\langle \cos(n\phi) \rangle \text{ for } n = 1, 2, 3$$

H1 Unfolded Data



- **Note: Calculations done $q_{\perp} \leq 3.0$ GeV**
- **Differences could be due to sample bin average within the fiducial cuts**
- **CT18A is also a TMD calculation, disagreement could also be in kinematics constraints**

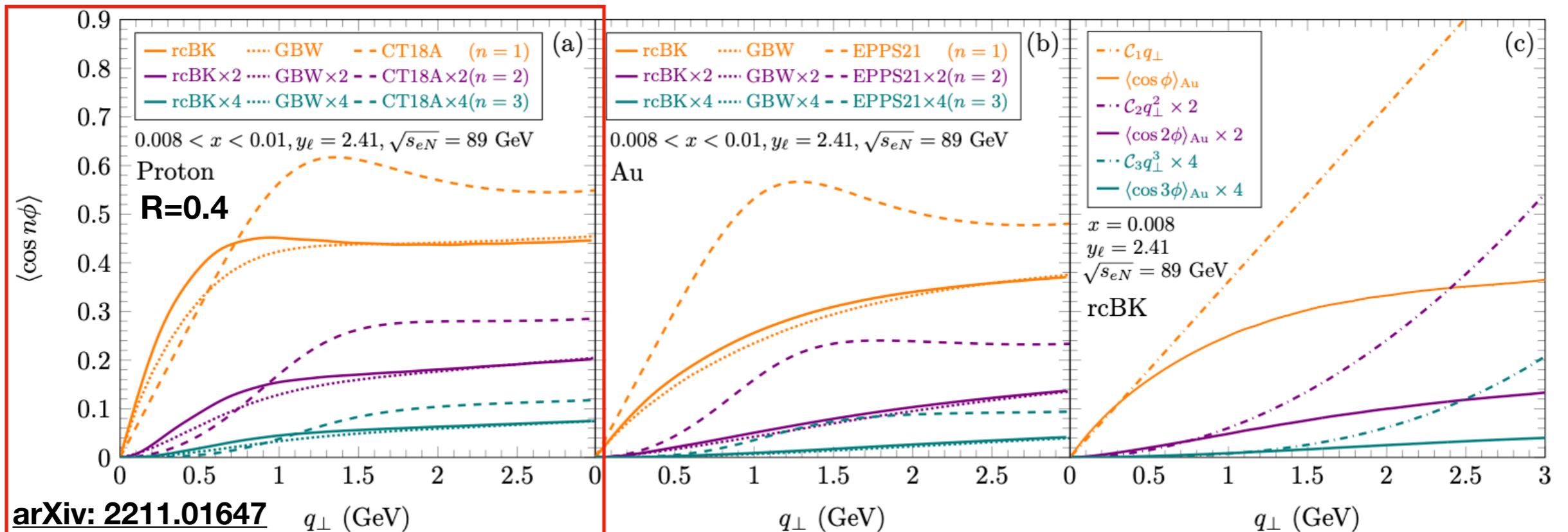
Two Sets of Calculations (Compare 2nd)



$$\vec{q}_\perp = \vec{k}_{\ell\perp} + \vec{k}_{J\perp}$$

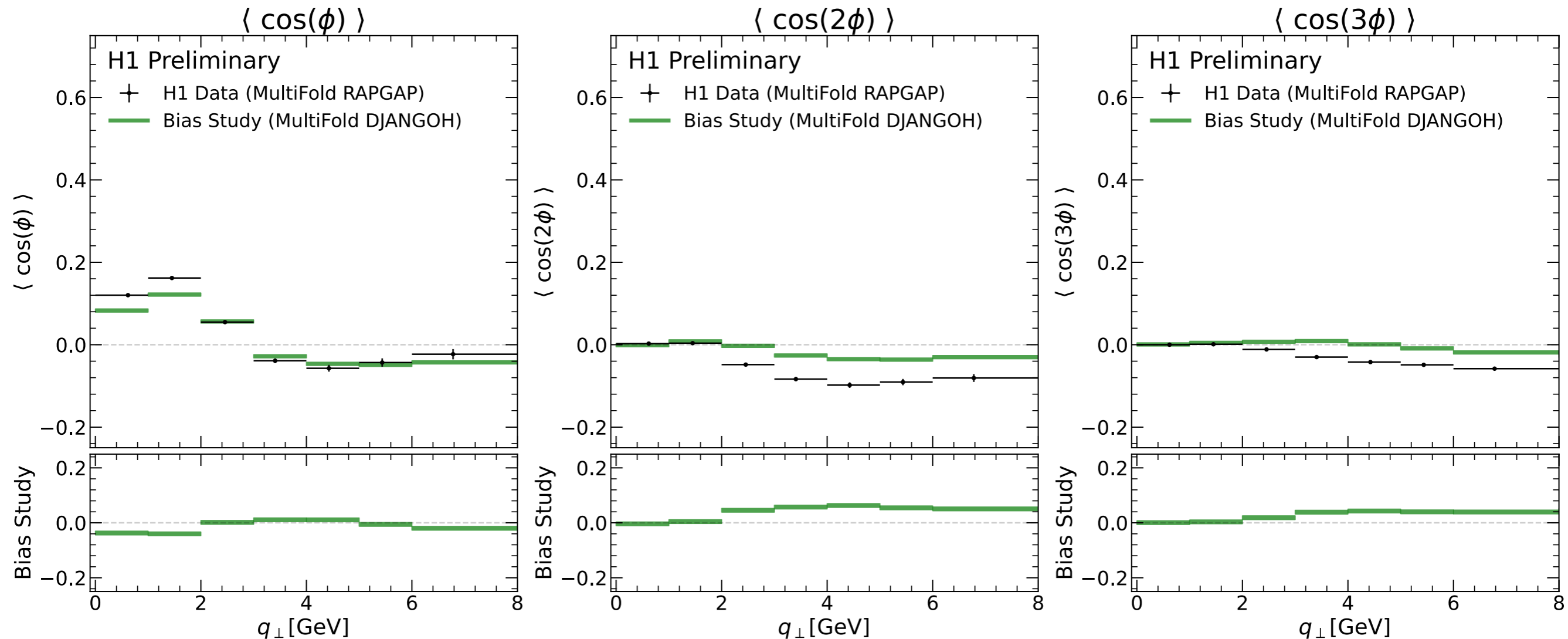
$$\vec{P}_\perp = (\vec{k}_{\ell\perp} - \vec{k}_{J\perp}) / 2$$

$\sqrt{s} = 140 \text{ GeV}, P_\perp = 20 \text{ GeV},$
 $y_l = 1.5, Q = 25 \text{ GeV}$
Radiative corrections
enhanced $\propto (\alpha_s \ln^2 P_\perp^2 / q_\perp^2)^n$
Soft Gluon Resummation



Harmonics of saturation with inputs from **GBW** model and **CT18A** PDF

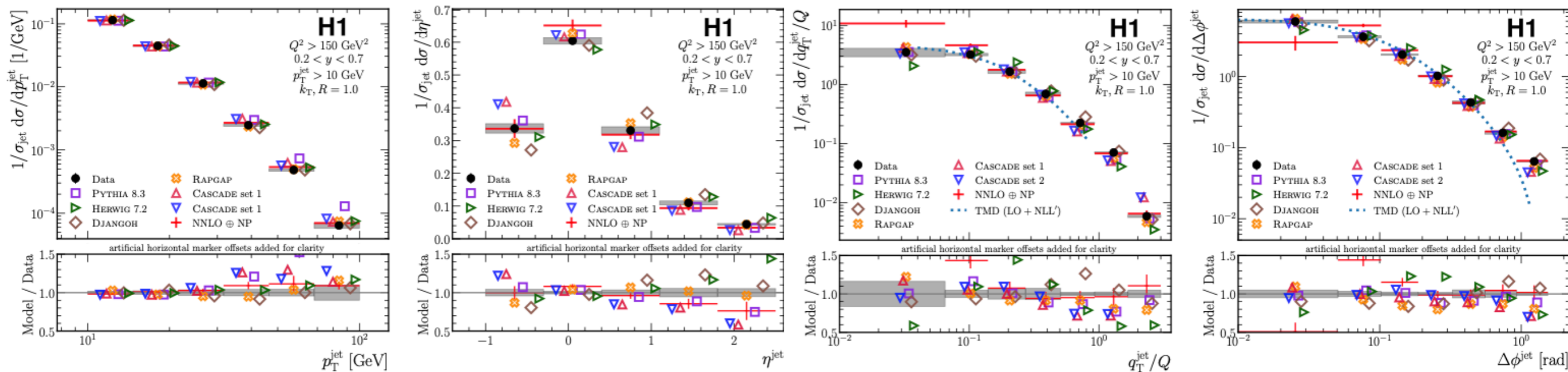
Investigation of Model Bias vs. q_{\perp} [GeV]



- Leading uncertainty is model bias in the unfolding for $\cos(2\phi)$ and $\cos(3\phi)$
- Difference in the result when unfolding using RAPGAP and DJANGO
- Reporting Abs. Errors; central values are very close to 0.0
- The Total Uncertainty is quite stable between harmonics

Backup Further Background

- Machine learning (OmniFold) is used to perform an 8-dimensional, unbinned unfolding.
- Use the 8-dimensional result to explore the Q^2 dependence and any other observables that can be computed from the electron-jet kinematics



**Extracted from the same phase-space as Yao's analysis,
but reporting a different observable**

OmniFold

$$1. \quad \omega_n(m) = \nu_{n-1}^{\text{push}}(m) L[(1, \text{Data}), (\nu_{n-1}^{\text{push}}, \text{Sim.})](m)$$

$$\nu_{n-1}(t) = \nu_n^{\text{push}}(m)$$

- Detector level simulation is weighted to match the data
- $L[(1, \text{Data}), (\nu_{n-1}^{\text{push}}, \text{Sim.})](m)$ approximated by classifier trained to distinguish the *Data* and *Sim.*

$$2. \quad \nu_n(t) = \nu_0(t) L[(\omega_n^{\text{pull}}, \text{Gen.}), (\nu_0, \text{Gen.})](t)$$

$$\omega_n^{\text{pull}}(t) = \omega_n(m)$$

- Transform weights to a proper function of the generated events to create a new simulation
- $L[(\omega_n^{\text{pull}}, \text{Gen.}), (\nu_{n-1}, \text{Gen.})](t)$ approximated by classifier trained to distinguish Gen. with *pulled* weights from Gen. using $\text{weights}_{\text{old}} / \text{weights}_{\text{new}}$

Each iteration of step 2 learns the correction from the original ν_0 weights

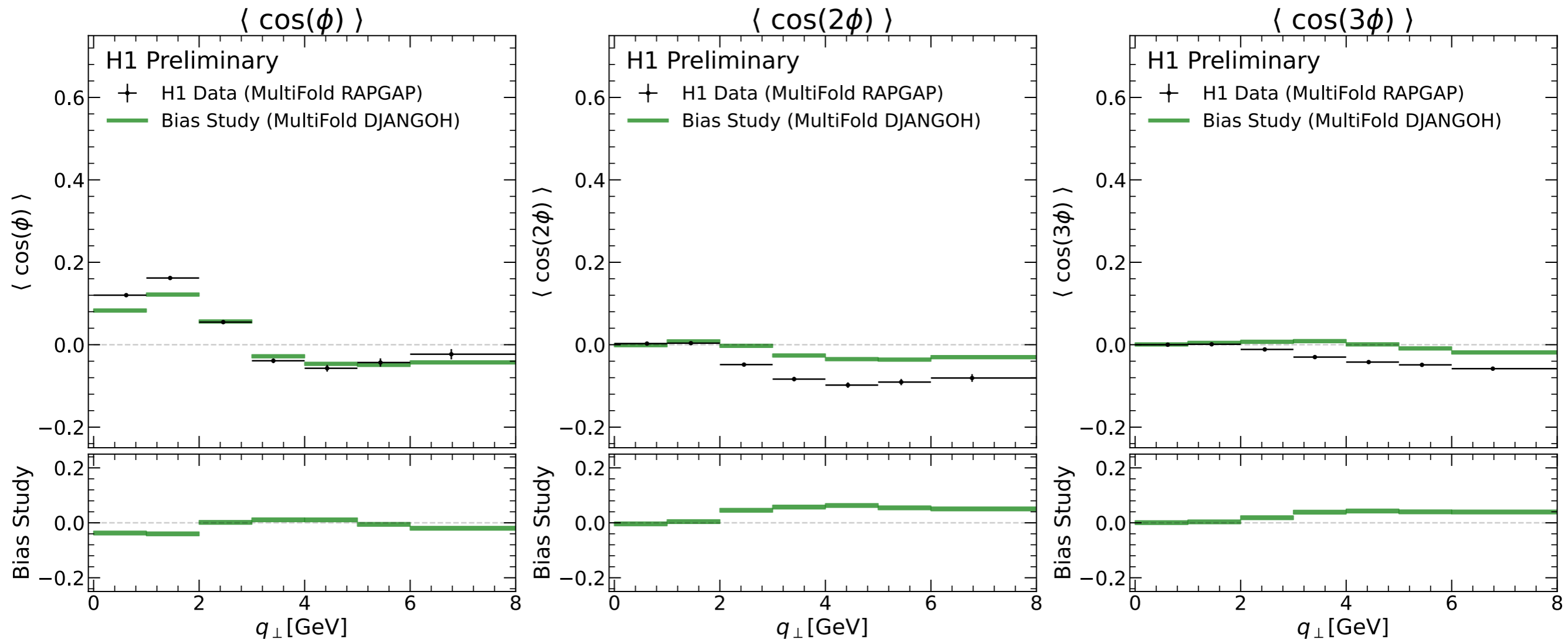
Advantage: Easier implementation, no need to store previous ν_n model

Disadvantage: Learning correction from ν_0 is more computationally expensive

Systematic Uncertainties

- Model Dependence:
 - The bias of the unfolding procedure is determined by taking the difference in the result when unfolding using RAPGAP and DJANGO
 - The two generators have different underlying physics, thus providing a realistic evaluation of the procedure bias
- QED Radiation Corrections
 - Difference of correction between RAPGAP and DJANGO
 - Take RAPGAP with and without QED corrections
 - Take DJANGO with and without QED corrections
- Systematic uncertainties are determined by varying an aspect of the simulation and repeating the unfolding
 - These values detail the magnitude of variation:
 - HFS-object energy scale: $\pm 1 \%$
 - HFS-object azimuthal angle: ± 20 mrad
 - Scattered lepton azimuthal: ± 1 mrad
 - Scattered lepton energy: $\pm 0.5 - 1.0 \%$

Investigation of Model Bias vs. q_{\perp} [GeV]

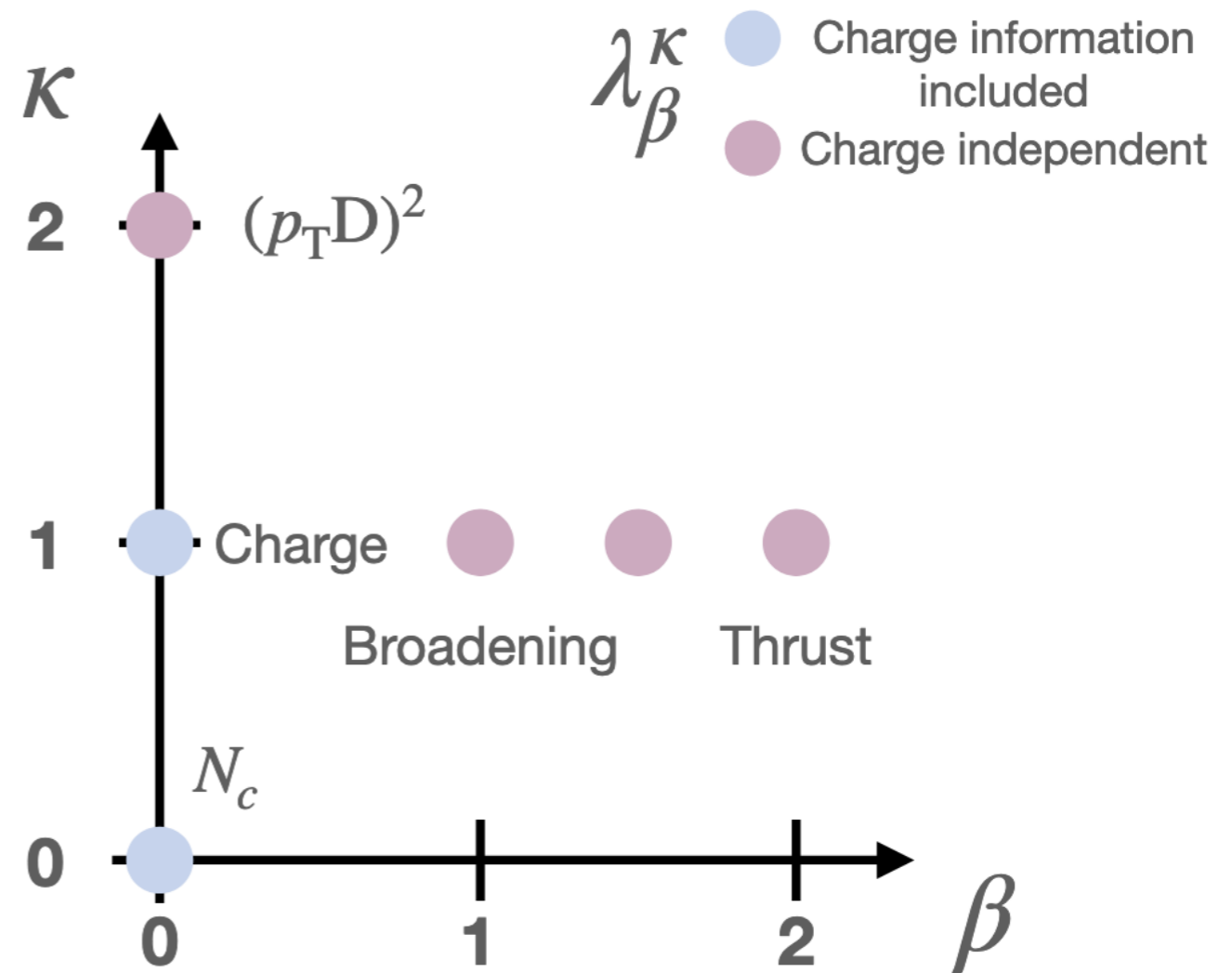


- Leading uncertainty is model bias in the unfolding for $\cos(2\phi)$ and $\cos(3\phi)$
- Difference in the result when unfolding using RAPGAP and DJANGO
- Reporting Abs. Errors; central values are very close to 0.0
- The Total Uncertainty is quite stable between harmonics

Jet Substructure Observables

Description of the jet substructure observables measured in this work.

Name/Symbol	Observable definition	Charge used
Logarithm of jet broadening Intermediate observable	$\ln(\lambda_1^1)$ $\ln(\lambda_{1.5}^1)$	No
Logarithm of jet thrust	$\ln(\lambda_2^1)$	
Momentum dispersion $p_T D$	$\sqrt{\lambda_0^2}$	
Charged particle multiplicity N_c	$\tilde{\lambda}_0^0$	Yes
Jet charge Q_1	$\tilde{\lambda}_0^1$	



IBU Generalization

IBU

$$t_j^{(n)} = \sum_i \Pr_{n-1}(\text{truth is } j | \text{measure } i) \Pr(\text{measure } i)$$
$$= \sum_i \frac{R_{ij} t_j^{(n-1)}}{\sum_k R_{ik} t_k^{(n-1)}} \times m_i$$

**Continuous
Generalization**

$$\nu_1(t) p_{\text{Gen}}(t) = \int dm' p_{\text{Gen|Sim}}(t|m') p_{\text{Data}}(m')$$

**Using Classifiers that
approximate the
Likelihood ratio**

$$L[(w, X), (w', X')](x) = \frac{p_{(w, X)}(x)}{p_{(w', X')}(x)}$$

Both converge to maximum likelihood estimate of particle-level distribution

Cross Section & ϕ

$$\frac{d^5 \sigma^{ep \rightarrow e' q X}}{dy_\ell d^2 P_\perp d^2 q_\perp} = \sigma_0^{eq} x f_q(x) \delta^{(2)}(q_\perp)$$

**Gluon Matrix
Element**

$$\mathcal{M}^{\mu\nu}(x, k_\perp) = \int \frac{d\xi^- d^2 \xi_\perp}{P^+ (2\pi)^3} e^{-ixP^+ \xi^- + i\vec{k}_\perp \cdot \vec{\xi}_\perp} \quad ($$

$$\times \langle P | F_a^{+\mu}(\xi^-, \xi_\perp) \mathcal{L}_{vab}^\dagger(\xi^-, \xi_\perp) \mathcal{L}_{vbc}(0, 0_\perp) F_c^{\nu+}(0) | P \rangle$$

**Integration over
emitted gluon
phase space**

$$g^2 \int \frac{d^3 k_g}{(2\pi)^3 2E_{k_g}} \delta^{(2)}(q_\perp + k_{g\perp}) C_F S_g(k_J, p_1)$$

$$= \frac{\alpha_s C_F}{2\pi^2 q_\perp^2} \left[\ln \frac{Q^2}{q_\perp^2} + \ln \frac{Q^2}{k_{\ell\perp}^2} + c_0 + 2c_1 \cos(\phi) + 2c_2 \cos(2\phi) + \dots \right],$$

**Fourier Coefficient
(Introduces ϕ
dependance)**

$$c_n = \ln \frac{1}{R^2} + f(n) + g(nR),$$

$$f(n) = \frac{2}{\pi} \int_0^\pi d\phi (\pi - \phi) \frac{\cos \phi}{\sin \phi} (\cos n\phi - 1),$$

$$g(nR) = \frac{4}{\pi} \int_0^1 \frac{d\phi}{\phi} \tan^{-1} \frac{\sqrt{1 - \phi^2}}{\phi} [1 - \cos(nR\phi)]$$

$$= \frac{n^2 R^2}{4} {}_2F_3 \left(1, 1; 2, 2, 2; -\frac{n^2 R^2}{4} \right).$$

Differential Cross Section

- Back-to-back electron-jet production from ep collision,

$$e(l) + p(P) \rightarrow e(l') + J_q(p_J) + X$$

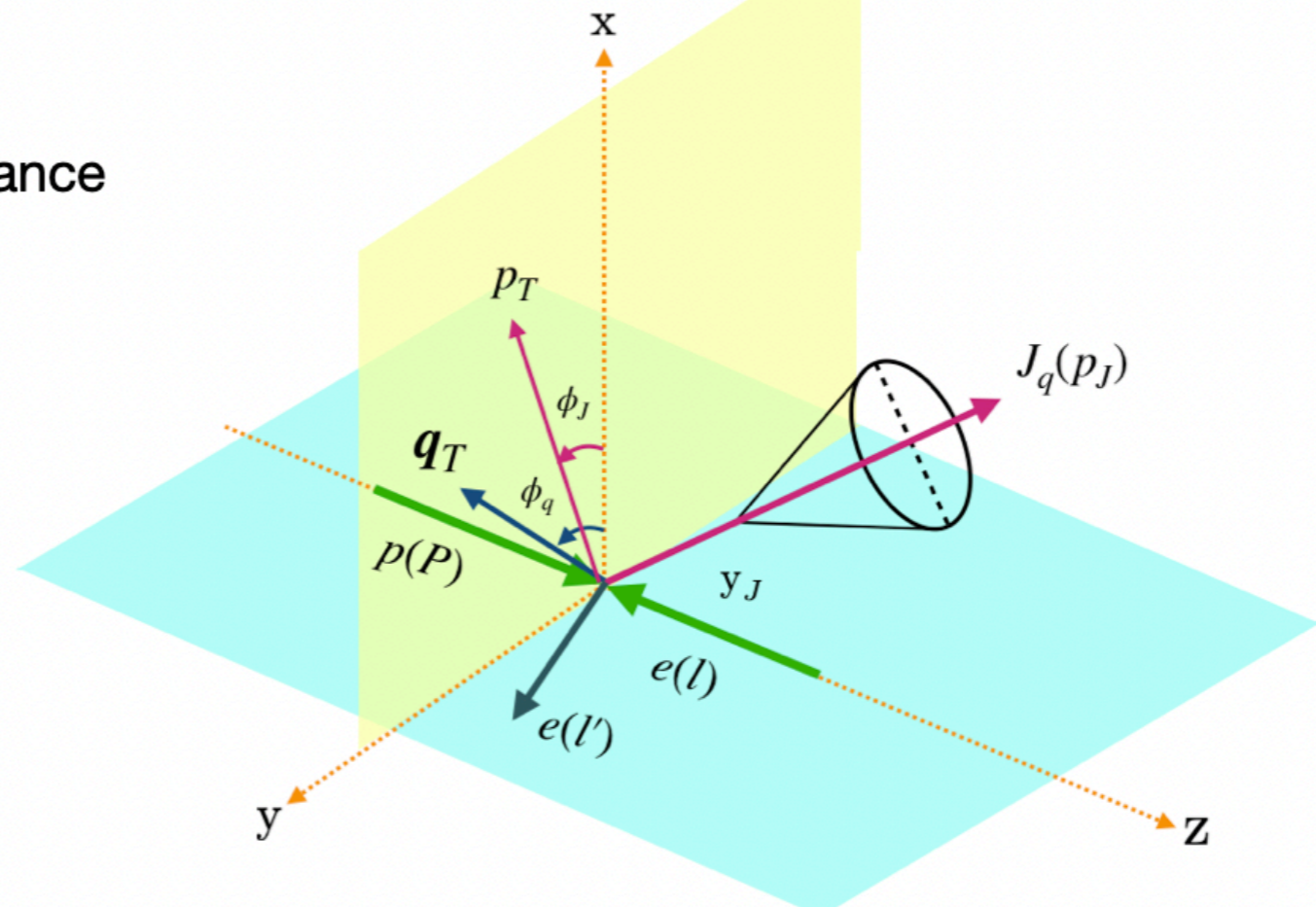
$$\frac{d\sigma}{d^2\mathbf{p}_T dy_J d\phi_J d^2\mathbf{q}_T} = \frac{d\sigma}{2\pi d^2\mathbf{p}_T dy_J q_T dq_T} \left[1 + 2 \sum_{n=1}^{\infty} v_n(p_T, y_T) \cos(n(\phi_q - \phi_J)) \right]$$

q_T : transverse momentum imbalance

$$\mathbf{q}_T = \mathbf{l}'_T + \mathbf{p}_{JT}$$

p_T : jet transverse momentum

y_J : jet rapidity



Note: slightly different angle definition, but background still applies]

